Stanczyk M. Alexander (Orcid ID: 0000-0001-6010-5750)
Weinberg Zara (Orcid ID: 0000-0001-7176-038X)
Traynor John (Orcid ID: 0000-0002-1849-8316)

The delta opioid receptor positive allosteric modulator BMS 986187 is a G protein biased allosteric agonist

Running title: Biased allosteric agonist at the delta-opioid receptor

M. Alexander Stanczyk[1], Kathryn E. Livingston[1], Louise Chang[1], Zara Weinberg[1], Manoj Puthenveedu[1], John R. Traynor[1*]

[1] Department of Pharmacology and Edward F. Domino Research Center, University of Michigan Medical School, Ann Arbor, Michigan

***Correspondence:**

John Traynor, Department of Pharmacology, University of Michigan Medical School,

1150 West Medical Center Drive, 2301 MSRB 3, Ann Arbor, MI, 48109. E-mail: jtraynor@umich.edu

This is the author manuscript accepted for publication and has undergone full peer review but has not been through the copyediting, typesetting, pagination and proofreading process, which may lead to differences between this version and the Version of Record. Please cite this article as doi: 10.1111/bph.14602

Word Count

Introduction	692
Results	1929
Discussion/conclusions	1395
Total	4016

Background and Purpose: The delta opioid receptor (DOPr) is an emerging target for the management of chronic pain and depression. Studies have highlighted the potential of biased signaling, the preferential activation of one signaling pathway over another downstream of DOPr, to generate a better therapeutic profile. BMS 986187 is a recently discovered positive allosteric modulator (PAM) of the DOPr. Here we ask if BMS 986187 can directly activate the receptor from an allosteric site in the absence of orthosteric ligand and if a signaling bias is generated.

Experimental Approach: Using various clonal cell lines expressing DOPr we investigated the effects of BMS 986187 on events downstream of DOPr by measuring G protein activation, β-arrestin 2 recruitment, receptor phosphorylation, loss of surface receptor expression, ERK 1/2 phosphorylation, and receptor desensitization.

Key Results: BMS 986187 is a G protein biased allosteric agonist relative to β-arrestin 2 recruitment. Despite showing direct and potent G protein activation, BMS 986187 has a low potency to recruit β-arrestin 2. Data suggests this is the result of limited receptor phosphorylation and ultimately leads to low receptor internalization and a slower onset of desensitization.

Conclusions and Implications: This is the first evidence of biased agonism mediated through direct binding to an allosteric site on an opioid receptor in the absence of occupancy of the orthosteric site. Our data suggests that agonists targeting DOPr, or indeed any GPCR, through an allosteric site may be a novel way to promote signaling bias and thereby potentially produce a more specific pharmacology than can be observed by activation *via* the orthosteric site.

Abbreviations:

AC (adenylyl cyclase); CFP (cyan fluorescence protein); DOPr (Delta opioid receptor); EKAR (extracellular signal-regulated kinase activity reporter); FRET (fluorescence resonance energy transfer); GDP: (guanosine 5' -diphosphate); GPCR (G protein coupled receptor); GTPγS (guanosine-5'-O-(3-thio) triphosphate); MOPr (mu opioid receptor); NTI (Naltrindole); PAM (positive allosteric modulator).

Bullet point summary

What is already known:

- The DOPr is a potential drug target for the management of pain and depression

- BMS 986197 is a positive allosteric modulator of the DOPr

What this study adds:

- BMS 986187 directly activates DOPr's *via* an allosteric site
- The direct DOPr agonism of BMS 986187 is biased for G-protein activation over β-arrestin recruitment

Clinical significance:

- DOPr orthosteric agonists can be proconvulsant
- Targeting DOPr with a G-protein biased allosteric agonist may be a potentially safer therapeutic strategy

1. Introduction

Chronic pain and depression are two of the most common medical ailments experienced worldwide and are often comorbid. For example, an estimated 25% of the United States population (75 million people) experience moderate to severe chronic pain (Reinke, 2014), while an estimated 15-20% experience depression (Kessler and Bromet, 2013). Opioid analgesics that target the mu opioid receptor (MOPr) are the most widely prescribed drugs for both chronic and acute pain, but suffer from serious side effects including respiratory depression and abuse

liability (McNicol et al., 2017; Przewłocki & Przewłocka, 2001). Treatments for depression are varied, but under the best circumstances only an estimated 50% of patients show full remission (Rush et al., 2006). Mounting evidence suggests that agonists targeting the delta opioid receptor (DOPr), a G protein coupled receptor (GPCR), are effective in preclinical models of chronic pain and depression and could provide for new therapies (Jutkiewicz et al., 2005; Bie and Pan, 2007; Cahill et al., 2007; Kabli and Cahill, 2007; Saitoh and Yamada, 2012).

The development of DOPr agonists, such as BW373U86, SNC80 and related compounds, as medications has been limited due to on-target side effects, namely a propensity to cause convulsions and the rapid development of tolerance both in rodent and non-human primate models (Jutkiewicz et al., 2005; Danielsson et al., 2006; Pradhan et al., 2012; Lutz, Pierre-Eric and Brigitte, 2014). Until recently, all compounds developed as DOPr agonists targeted the orthosteric site on the receptor. However, the discovery of allosteric modulators that act at DOPr, in particular BMS 986187 (Burford et al., 2015), presents an opportunity to interrogate this receptor in a novel way. An allosteric modulator is a compound that binds to a site on a GPCR other than the endogenous ligand or orthosteric site, and by doing so modulates the affinity and/or efficacy of an orthosteric ligand. Allosteric modulators can either be positive (PAM), negative (NAM), or silent (SAM) with regards to their effect on orthosteric ligands (Conn et al., 2010; Keov et al., 2011). Modulators may also possess direct intrinsic pharmacological activity themselves. Such compounds are commonly referred to as “ago-

PAM's" or "ago-NAM's" depending on the nature of this activity (Langmead and Christopoulos, 2006; Kenakin, 2007).

One potential benefit of allosteric modulators is to engender biased agonism, or functional selectivity (Kenakin and Christopoulos, 2013). Biased agonism is the preferential activation, or inhibition, of certain downstream signaling cascades over others, classically G protein activation over β-arrestin recruitment (Whalen et al., 2011; Kenakin et al., 2012; Kenakin and Christopoulos, 2013; Schmid et al., 2017). Thus, in theory, a drug could promote downstream effectors associated with beneficial actions while bypassing the effectors associated with the unwanted effects. Multiple studies have suggested biased agonism stemming from orthosteric activation of the DOPr, although pertinent rigorous bias calculations are rarely performed (Audet et al., 2008), see for review (Pradhan et al., 2012). Evidence suggests that β-arrestin 2 mediated internalization of the DOPr might be associated with some of the negative effects of DOPr agonists. Indeed, a number of ligands that fail to internalize the DOPr such as ARM390, despite potent G protein activation, have shown reduced tolerance (Pradhan et al., 2009, 2010, 2012) and reduced propensity to cause convulsions (Pradhan et al., 2011) in animal models. This suggests an agonist that preferentially activates G protein over β-arrestin 2 recruitment may have reduced on-target side effects that have limited the utility of other DOPr ligands, such as SNC80. However, this does conflict with recent experiments in β-arrestin knockout mice suggesting that β-arrestin 2 recruitment does not contribute significantly to the onset of convulsions (Dripps et al., 2017).

To date no studies have examined the role allosteric modulation plays in functional selectivity at the DOPr. BMS 986187 shows probe dependence at the DOPr and our prior work suggests it may be a directly acting allosteric agonist as evidenced by its ability to inhibit of adenylyl cyclase (AC) in the absence of orthosteric agonist (Burford et al., 2015). To this end, we set out to elucidate the nature of this ago-PAM activity. We found that BMS 986197 is an allosteric agonist with biased signaling towards G protein pathways over the recruitment of β-arrestin 2.

2. Methods

2.1. Materials

Guanosine-5'-O-(3-[^{35}S]thio)triphosphate (GTPγ^{35}S) and [^{3}H]diprenorphine were from Perkin Elmer Life and Analytical Sciences (Boston, MA, USA). BMS 986187 was synthesized and characterized as previously described (Burford et al., 2015). Naltrindole, Naloxone, TAN-67, DPDPE, SNC80, protease inhibitor cocktail, guanosine diphosphate, p-nitrophenyl phosphate, M1 mouse anti-FLAG antibody (Cat# F3040, RRID:AB_439712) and M2 mouse anti-FLAG antibody conjugated to alkaline phosphatase (Cat# A9469, RRID:AB_439699 were from Millipore-Sigma (St Louis, MO, USA). Goat-anti-rabbit (Cat# sc-2004, RRID:AB_631746) or mouse (Cat# sc-2005, RRID:AB_631736) anti-bodies conjugated to horseradish peroxidase (HRP) were from Santa Cruz Biotechnology (Santa Cruz, CA, USA) and rabbit anti- phospho-

Ser363-DOPr-opioid receptor antibody (Cat # 3461 RRID:AB_2768155) from Cell Signaling (Danvers, MA, USA). β-arrestin 2-GFP cDNA was a gift from Marc Caron (Duke University, Durham, NC, USA). Poly-D-lysine coated 24-well plates and poly-D-lysine coated 12 mm, no. 1 coverslips were from BD Biosciences (San Jose, CA, USA). EcoLume scintillation cocktail and ultrapure formaldehyde were obtained from MP Biomedicals (Aurora, OH, USA) and Polysciences Inc. (Warrington, PA, USA), respectively. ProLong Gold antifade reagent, Alexa 594 goat anti-mouse IgG (Thermo Fisher Scientific, catalog # A-11032, RRID AB_2534091) and Lipofectamine 2000 were from Invitrogen (Carlsbad, CA, USA). One-Glo solution was purchased from Promega (Madison, WI, USA). SuperSignal chemiluminescent substrate was purchased from ThermoFisher (Waltham, MA, USA).

2.2. Animals

All animal care and experimental procedures complied with the US National Research Council's Guide for the Care and Use of Laboratory Animals (Council, 2001). Animal studies are reported in compliance with the ARRIVE guidelines (Kilkenny et al., 2010; McGrath and Lilley, 2015). Male mice were used for all experiments. C57BL/6N (RRID:MGI:5659255) mice were obtained from Envigo (formerly Harlan, Indianapolis, IN). The *Oprd1*^{tm1Kff}/J mouse strain (Oprd1tm1Kff/J, RRID:IMSR_JAX:007557) was obtained from The Jackson Laboratory (Bar Harbor, Maine, https://www.jax.org/strain/007557; Filliol et al., 2000). Mice were group-housed with a maximum of five animals per cage in clear polypropylene cages with corn cob bedding and nestlets as enrichment. For breeding of the *Oprd1*^{tm1Kff}/J mice heterozygote pairs were

employed. Mice had free access to food and water at all times. Animals were housed in pathogen-free rooms maintained between 68 and 79°F and humidity between 30 and 70% humidity with a 12 h light/dark cycle with lights on at 07:00 h.

2.3. Cell Lines.

Human Embryonic Kidney (HEK293, RRID:CVCL_0045) cells stably expressing a tTA-dependent luciferase reporter and a β-arrestin 2-TEV fusion gene (HTLA cells; Thermo-Fisher Scientific) were maintained in DMEM supplemented with 10% FBS, 1% penicillin and 100 μg/ml streptomycin, 2 μg/ml puromycin and 100 μg/ml hygromycin B at 37°C and 5% CO_2. HEK293 (ATCC Cat# CRL-1573, RRID:CVCL_0045) cells expressing N-terminally FLAG tagged human-DOPr (HEK-hDOPr) were cultured in DMEM containing 10% FBS and 1% penicillin and streptomycin and maintained in 0.8 mg/ml G418. HEK 293 cells stably expressing an N-terminally FLAG-tagged variant of hDOPr for ERK 1/2 imaging studies were generated as previously described and maintained in DMEM supplemented with 10% FBS (Shiwarski et al., 2017). CHO (ATCC Cat# CCL-61, RRID:CVCL_0214) cells stably expressing wild-type human-DOPr (CHO-hDOPr) were grown in DMEM containing 10% FBS and 1% penicillin and streptomycin and maintained in 0.4 mg/ml G418 as previously described (Burford et al., 2015)

2.4. Membrane Homogenate Preparations.

2.4.1. Cells were harvested and membrane homogenates prepared as previously described (Clark et al., 2003). Briefly, cells were washed with ice-cold phosphate buffered saline, pH 7.4

and detached from plates by incubation in harvesting buffer (0.68 mM EDTA, 150 mM NaCl, and 20 mM HEPES at pH 7.4) and pelleted by centrifugation at 200g for 3 minutes. Cells were resuspended in ice-cold 50mM Tris (pH 7.4), homogenized using a Tissue Tearor (Dremel; Mount Prospect, IL, USA), and centrifuged at 20,000g at 4^{o}C for 20 min. The pellet was then resuspended, homogenized, and centrifuged a second time. This final pellet was resuspended in ice-cold 50 mM Tris (pH 7.4) and homogenized using a glass dounce to give a protein concentration of 0.5-1.5 mg/mL and stored at -80°C. Protein concentration was determined using the bicinchoninic acid quantification method (BCA) with BSA serving as the standard.

2.4.2. For brain homogenates, mice (8 to 12 weeks of age) were euthanized by cervical dislocation. Whole brain tissue, from the optic chiasmus forward, was removed immediately and chilled in ice-cold 50 mM Tris base, pH 7.4. previously described (Lester and Traynor, 2006). Final membrane pellets were resuspended in 50 mM Tris base, pH using BCA assay with BSA as the standard.

2.5. Stimulation of GTPγ^{35}S Binding.

Agonist stimulation of GTPγ^{35}S binding was measured as described previously (Clark et al., 2003). Homogenates of HEK cells expressing FLAG-tagged-hDOPr, CHO cells expressing wild-type hDOPr or mouse brain (15-20 μg/well) were incubated in "GTPγS buffer" (50 mM Tris-HCl, 100 mM NaCl, 5 mM $MgCl_2$, pH 7.4) containing 0.1 nM GTPγ^{35}S, 30 μM guanosine diphosphate (GDP) and varying concentrations of BMS 986187, or DOPr agonists for 1h in a

shaking water bath at 25°C. The reaction was terminated by vacuum filtration through GF/C filters using a Brandel harvester and washed five times with ice-cold GTPγS buffer. Filters were dried, and following the addition of EcoLume scintillation cocktail, counted in a Wallac 1450 MicroBeta Liquid Scintillation and Luminescence Counter (Perkin Elmer). The level of GTPγ^{35}S binding was expressed as fmols bound/mg protein or by comparison with the full DOPr agonist SNC80 at 10 μM to account for variability between membrane preparations.

2.6. DOPr Internalization.

As described previously (Bradbury et al., 2009), FLAG-tagged HEK-hDOPr cells were plated at a density of 0.5 x 10^6 cells per well in poly-D-Lysine coated, 24-well plates. When cells reached 80% confluency they were treated with vehicle (1% DMSO) or indicated drugs and rocked at room temperature for the indicated times. Cells were then washed three times with ice-cold tris-buffered saline (TBS) and fixed with 3.7% paraformaldehyde in TBS at room temperature for 15 min. After fixing, cells were washed three times with cold TBS and blocked at room temperature with 1% BSA in TBS for 60 min. Following block, cells were washed two times with TBS and incubated with FLAG M2-Alkaline Phosphatase Antibody at a 1:625 dilution for 60 min. Cells were then washed five times with TBS and treated with p-nitrophenylphosphate for 8 min. The reaction was stopped with 3N NaOH and 200 μl from each well was transferred to a 96-well plate for reading at 405 nm on VERSAmax tunable microplate reader (Molecular Devices, Sunnyvale, CA). The percentage of internalized receptors was determined as loss of surface receptors using the following equation [1–(Drug O.D.–Background

O.D./ Control O.D.–Background O.D.) x 100]. Background was determined as the absorbance of non-transfected HEK cells and control was the absorbance of cells incubated in the absence of drug.

2.7. β-Arrestin 2 Recruitment.

2.7.1 Confocal Microscopy

Recruitment of β-arrestin 2 in FLAG-tagged HEK DOPr cells was performed as described previously (Bradbury et al., 2009). Briefly, cells were seeded into 24-well plates containing Poly-D-Lysine coated glass coverslips. Cells were transfected using Lipofectamine 2000 with 0.4 μg of β-arrestin 2-GFP cDNA and incubated for 48 h, then treated with either vehicle, 10 μM SNC80 or 10 μM BMS 986187 for 5 min. Following fixation with 3.7% paraformaldehyde, cells were incubated with M2 Mouse Anti-FLAG primary antibody followed by AlexFluor 594 Goat Anti-Mouse secondary antibody. Images were obtained using a NikonA1R Confocal Microscope and quantified using Image J software (National Institutes of Health) (ImageJ, RRID:SCR_003070).

2.7.2 Presto-Tango Arrestin Recruitment

For the PRESTO-TANGO assay HTLA cells at 15,000 cells/well were transfected with plasmids (20ng) encoding FLAG-tagged hDOPr-TANGO (OPRD1-TANGO; Thermo-Fisher Scientific) using Lipofectamine 2000, and plated in Greiner Bio-One cell culture micro-plates. After 24 h, cells were treated with the indicated drug at the indicated concentrations. After 48

h, One-Glo solution was added to each well and luminescence was measured using a Pherastar plate reader (BMG Labtech, Germany). Data were normalized to percent of standard full agonist (10 μM SNC80) to account for variability between assays in plating and transfection efficiency.

2.8. ERK 1/2 Phosphorylation.

HEK 293 cells stably expressing an FLAG-tagged hDOPr were transiently transfected with the extracellular signal-regulated kinase activity reporter cEKAR (Fritz et al., 2013). ERK activity in response to SNC80 and BMS 986187 was assessed as previously described (Weinberg et al., 2017). Briefly, cells were plated at low density, allowed to grow for two days, and then serum starved for 4 h. Cells were labeled with Alexa Fluor 647 anti-mouse M1 antibody for 10 min. Single-cell fluorescence for cyan fluorescent protein (CFP; 405 nm excitation, 470/50 emission filter), FRET (405nm excitation, 530lp emission filter), and M1 (647 nm excitation, 700/75 emission) was collected every 30 s for 22.5 min, with addition of drug (1 μM SNC80 or 10 μM BMS 986187) occurring after 2.5 min of no-treatment baseline. The ratio of FRET to CFP fluorescence was calculated for each cell on a frame-by-frame basis and normalized to the average ratio during baseline. For calculating total response, the mean area under the curve was taken for the vehicle condition, and that mean was subtracted from the individual area under the curve for each cell in the treatment conditions. Each experiment was conducted using the same batch of transiently transfected cells from the same stable cell line and passage number and

carried out on the same day under all conditions (vehicle, SNC80, BMS-986187) to ensure that any non-responding cells were represented equally across treatment conditions.

2.9. Western blot for phosphoSer363.

As described previously (Bradbury et al., 2009), HEK cells stably expressing FLAG-tagged hDOPr were plated at a density of 0.5 x 10^6 cells per well in poly-D-Lysine coated, 24-well plates and experiments were performed when cells were at 80% confluency. Cells were treated with vehicle (1% DMSO), TAN-67, DPDPE, SNC80 or BMS 986187 for 1 h. Cells were then rinsed with phosphate buffered saline (PBS) and lysates were collected with RIPA buffer (50 mM Tris, pH 7.4, 150 mM NaCl, 1% Triton X-100, 1% sodium deoxycholic acid, 0.1% sodium dodecyl sulfate (SDS)) plus protease inhibitor cocktail, 2 mM EDTA, 100 mM NaF, 100 mM phenylmethanesulfonyl fluoride, and 10 mM sodium orthovanadate. Lysates were then sonicated briefly and centrifuged at 10,000 g for 10 min. Equal amounts of protein samples were diluted in SDS sample buffer (62.5 mM Tris–HCl, pH 6.8, 2% SDS, 10% glycerol, 0.0008% bromophenol blue) and β-mercaptoethanol, loaded onto 10% polyacrylamide gels. Following transfer to nitrocellulose, membranes were blocked for 1 h with 5% non-fat dried milk in PBS then incubated with 1:1000 dilution of rabbit anti-phosphorylated δ-opioid receptor antibody overnight at 4˚C. Membranes were washed and incubated with 1:10000 HRP-goat anti-rabbit IgG for 1 h. To probe total FLAG-DOPr, the membranes were stripped using mild stripping buffer (distilled water, pH 2.2, 1.5% glycine, 0.1% SDS, 1% Tween 20), washed, then blocked with 5% non-fat dried milk for 1 h. Following block, membranes were incubated with 1:1000

mouse-anti-FLAG for 1 h 5% non-fat dried milk in TBS-Tween containing 1mM $CaCl_2$. Membranes were washed and treated with 1:10000 HRP-goat-anti-mouse IgG for 1 h. Following wash, membranes were treated with 1:1 SuperSignal chemiluminescent substrate and bands were detected using the EpiChemi3 darkroom (UVP, Upland, CA, USA). Band intensity was quantitated using Image J (National Institutes of Health) and normalized to total hDOPr, as determined by FLAG staining, to account for any differences in total protein.

2.10. Receptor Desensitization

Desensitization was determined by incubating hDOPr CHO cells with either vehicle or drug for indicated time periods at 37˚C. Following incubation, cells were washed five times with PBS and membranes were prepared as described above. For the time course of desensitization, maximum GTPγ^{35}S binding was measured using 10 μM SNC80 in vehicle treated cells; drug treated conditions were expressed as percent of this maximal binding. For concentration response, GTPγ^{35}S binding elicited by SNC80 was measured in membranes pre-treated with either 500 nM SNC80, 10 μM BMS 986187 or vehicle for 30 min and expressed as fmol bound/mg of protein.

2.11. Analyses and statistical analyses

The data and statistical analyses comply with the recommendations on experimental design and analysis in pharmacology (Curtis et al., 2015). All *in vitro* assays were a mean of at least 5 separate preparations, except where stated, and each was run in duplicate or triplicate as given in

the relevant figure legend, to ensure the reliability of the single values. None of the *in vitro* biochemical experiments were performed or analyzed blinded

Data were graphed as individual experiments for analyses unless otherwise stated and statistical analysis was performed using Graphpad Prism 6.5. Concentration-effect curves were analyzed using a three-parameter curve fit with Hill Slopes set to 1.0. Maximal values were not constrained; minimum values were constrained to zero if contained in the 95% confidence intervals. For internalization, the GTPγ^{35}S assay and confocal microscopy, one-way ANOVA was performed and Tukey post hoc test for multiple comparisons applied if F was significant. The desensitization time course was analyzed by two-way ANOVA. Bias calculations were performed as described by Kenakin, (2017) as follows: For each ligand and respective response, individual experimental curves were used to calculate log(max/EC50). The difference in log(max/EC50) between arrestin recruitment and GTPγ^{35}S, Δlog(max/EC50), was then calculated. Individual results were combined to give means ± SEM values shown in Table 1. Finally, the differences between the Δlog(max/EC50) values for the reference ligand (DAMGO) and test ligand were calculated to give a $\Delta\Delta$log(max/EC50) values, the antilog of which is the bias factor.

For all analyses significance was set at 5% (0.05 p value).

Nomenclature of Targets and Ligands

Key protein targets and ligands in this article are hyperlinked to corresponding entries in http://www.guidetopharmacology.org, the common portal for data from the IUPHAR/BPS Guide to PHARMACOLOGY (Harding *et al.*, 2018), and are permanently archived in the Concise Guide to PHARMACOLOGY 2017/18 (Alexander *et al.*, 2017).

3. Results:

3.1. BMS 986187 stimulates GTPγ^{35}S *Binding* via DOPr

BMS 986187 has been shown to produce inhibition of forskolin-stimulated cAMP production in the absence of orthosteric ligand, demonstrating that it has direct agonist action *via* an allosteric site (Burford et al., 2015). However, inhibition of adenylate cyclase (AC) is a highly amplified signaling output and requires low efficacy in a compound, although it does require prior stimulation of heterotrimeric Gαi/o proteins. To demonstrate that BMS 986187 can directly stimulate DOPr to activate Gαi/o, we performed GTPγ^{35}S binding assays as previously described (Traynor and Nahorski, 1995) in HEK 293 cells expressing human DOPr (Figure 1A). BMS 986187 stimulated GTPγ^{35}S binding in a concentration dependent manner giving a potency value (EC_{50}) of 301 ± 85 nM. In brain homogenates from C57/BL6 mice the DOPr full agonist SNC80 produced GTPγ^{35}S binding with an EC_{50} of 203 ± 31 nM (Figure 1B). BMS 986187 also stimulated GTPγ^{35}S binding with a weaker potency (EC_{50} of 1681 ± 244 nM), but the maximal GTPγ^{35}S response to BMS 986187 was 38% greater than that produced by SNC80. To confirm the response to BMS 986187 was due to DOPr receptor activation we repeated the experiments in brain tissue from DOPr knockout mice. In brain homogenates from these mice a small degree

of BMS 986187 stimulated GTPγ^{35}S binding remained, representing 20% of the BMS 986187 response observed in tissue from wild type mice, with an EC_{50} of 600 ± 397 nM. In contrast, SNC80 produced no appreciable binding over baseline in DOPr knockout mice. These findings suggest that BMS 986187 activates G protein through the DOPr at physiological receptor expression levels while also eliciting a very low level of G protein activation through a non-DOPr mediated pathway.

3.2. BMS 986187 stimulates GTPγ^{35}S *binding through an Allosteric Site on DOPr*

Previous work has shown that BMS 986187 does not displace the antagonist ^{3}H-diprenorphine binding from the orthosteric site (Burford et al., 2015). To verify that the agonist action of BMS 986187 is not due to interaction at the orthosteric site, GTPγ^{35}S binding was performed in membranes from HEK hDOPr cells in the presence or absence of various concentrations of orthosteric antagonists. The DOPr antagonist naltrindole (NTI) (100 nM) reduced the maximal GTPγ^{35}S binding evoked by 10 μM BMS 986187 from 99 ± 6% to 51 ± 17 % (Figure 2A). Increasing the concentration of NTI by 100-fold (to 10 μM) caused no additional inhibition of BMS 986187-stimulated GTPγ^{35}S binding (50 ± 4%; Figure 2A). NTI (10 μM) alone failed to produce any appreciable stimulation of GTPγ^{35}S binding, consistent with its classification as a neutral antagonist (Tryoen-Toth et al., 2005). The partial loss of BMS 986187-stimulated GTPγ^{35}S binding was also observed in the presence of 10 μM of the non-specific opioid antagonist naloxone. Using CHO hDOPr cells as an alternative cell line, NTI showed a

concentration-dependent, but saturable, inhibition of BMS 986187 stimulation of GTPγ^{35}S binding with the lack of parallel shifts confirming the agonist action of the modulator is not due competition at the orthosteric site but rather due to negative cooperativity between the orthosteric and allosteric sites. To further verify this, we evaluated the effect of increasing concentrations of NTI on the maximal stimulation elicited by BMS 986187 and SNC80 using membranes from CHO hDOPr cells (Figure 2C). NTI showed a saturable inhibition of BMS 986187 stimulation of GTPγ^{35}S binding. In contrast SNC80- mediated stimulation of GTPγ^{35}S binding was fully inhibited by NTI, consistent with a competitive mechanism.

3.3. BMS 986187 causes a low level of DOPr internalization

Previous studies of the DOPr suggests that ligands with high efficacy at activating G protein while maintaining low efficacy at promoting receptor internalization, show reduced tolerance in animal models (Pradhan et al., 2009). To this end, we next sought to determine whether BMS 986187 would cause DOPr internalization relative to the orthosteric partial agonists TAN-67 and DPDPE and the full agonist SNC80. Preliminary studies indicated that 10 μM would be a maximal effect for all ligands and from initial time course studies (Figure 3A) we chose 1 h to evaluate and compare the ligands. Due to the small effect window data were pooled for analysis to provide maximum and EC_{50} values with 95% Confidence Intervals. BMS 986187 treatment resulted in low levels of internalization (7 [3.9-10.0] %) relative to TAN-67 (11 [5.2-16.2] %) < DPDPE (31 [17.7- 44.1] %) and SNC80 (33 [24.7- 40.9] %) with a potency order

TAN-67 (1.3 [0.15 – 11.0] nM) = SNC80 (3.7 [1.5-9.2] nM) > BMS968187 (94 [59 – 1007] nM) = DPDPE (212 [72- 623] nM).

To contrast the propensity of BMS 986187 to cause internalization with its ability to activate G protein at DOPr we measured the maximal GTPγ^{35}S binding by BMS 986187 and compared this with saturating concentrations (10 μM) of the partial agonist peptide DPDPE, the partial agonist TAN-67 and the full agonist SNC80, which was used as the standard. As shown in Figure 4B, BMS 986187 elicited 99% ± 6 of GTPγ^{35}S binding relative to SNC80 versus 63% ± 7 and 75% ± 6 for TAN-67 and DPDPE respectively. Thus BMS 986187 gives a greater level of G protein activation than DPDPE but a reduced level of internalization. Additionally, BMS 986187 affords a similar level of internalization as TAN-67 but stimulates a higher level of GTPγ^{35}S binding.

3.4. BMS 986187 is G protein biased relative to β-arrestin 2 recruitment

The fact that BMS 986187 affords greater GTPγ^{35}S stimulation that DPDPE and TAN-67, while causing a low level of DOPr internalization is indicative of ligand bias. Internalization of receptors is largely β-arrestin-dependent therefore in order to explore this further, we directly compared concentration responses for BMS 986187 and SNC80 to recruit β-arrestin 2 to DOPr and stimulate GTPγ^{35}S binding. BMS 986187 and SNC80 stimulated a similar level of GTPγ^{35}S binding in HEK hDOPr cells (Figure 5B), in agreement with our previous result (Figure 1A) although BMS 986187 was less potent (Table 1). In contrast, using the PRESTO-TANGO assay BMS 986187 recruited β-arrestin 2 very weakly up to 100 μM, the limit of solubility (Figure

5A). Extrapolation of the BMS 986187 concentration-response curve assuming a similar maximum to SNC80, afforded an EC_{50} for BMS 986187 of 579 μM. In comparison TAN-67 and DPDPE recruited similar levels of β-arrestin 2 as SNC80, although DPDPE (16.1 ± 8.0 μM) was much less potent than TAN-67 (327 ± 176 nM) or SNC80 (353 ± 141 nM). From these data the relative bias of BMS 986187 for GTPγ^{35}S stimulation over β-arrestin 2 recruitment was evaluated with SNC80 serving as a reference agonist using the log(max/EC_{50}) function as described by Kenakin (Kenakin, 2017) (Table 1). This shows BMS 986187 is G protein biased relative to β-arrestin 2 when compared to SNC80, with a bias factor of 82 (Table 1). It should be noted that the PRESTO-TANGO assay employs a chimeric DOPr receptor with a Vasopressin receptor tail, although the effect of this modification should be eliminated using SNC80 as a reference ligand (Kenakin, 2017). Utilizing this assay, we found DPDPE to be biased towards G protein compared with SNC80 with a calculated bias factor of 11 (Table 1). This is similar to the bias of DPDPE compared to SNC80 of 6, calculated using the same equation from data in Chiang et al., 2016, who employed a complementation assay for β-arrestin recruitment in CHO cells. Moreover, the bias of BMS986187 fits with the change in ligand order when comparing internalization with GTPγ^{35}S binding (Fig 4), and the PRESTO-TANGO assay has been previously used in studies of receptor bias (Che et al., 2018).

To confirm the low degree of β-arrestin 2 recruitment to DOPr by BMS 986187, we performed confocal microscopy in FLAG tagged HEK DOPr cells transfected with 0.4 μg β-arrestin 2 GFP as shown in Figure 6. Cells were incubated for 5 min with 10 μM of either

SNC80 or BMS 986187, a saturating concentration for G protein activation. β-arrestin 2 localization was then quantified as a ratio of fluorescent intensity at the cell membrane divided by the cytoplasmic intensity using line scan analysis. Consistent with the findings in Figure 5B and published literature (Chiang et al., 2016), SNC80 afforded significant translocation of β-arrestin 2 to the plasma membrane, however, localization in cells treated with BMS 986187 was not significantly different from baseline. This suggests the maximal β-arrestin 2 recruitment in response to BMS986187 is much less than recruited by SNC80, so we re-calculated the bias factor assuming the 100 μM data point in Fig. 5A (the point of solubility) was the maximal effect; this calculation yielded a bias factor of 34 (Table 1).

3.5. BMS 986187 shows low levels of ERK 1/2 activation

Agonists at opioid receptors have been shown to signal through ERK 1/2 via both G protein and β-arrestin mediated pathways and previous work has shown that BMS 986187 acting as a PAM can increase the potency of orthosteric DOPr agonists in promoting ERK 1/2 phosphorylation (Burford et al., 2015). However, BMS 986187 (10 μM) alone failed to elicit significant ERK1/2 phosphorylation relative to vehicle in HEK hDOPr cells, whereas SCN80 (1 μM) afforded robust phosphorylation of ERK/12 (Figure 7). As expected, we observed SNC80-promoted DOPr internalization (Figure 7 A), but also saw internalization at later time points in approximately 50 % of cells treated with BMS 986187 (Figure 7 A). A similar percentage of vehicle treated cells showed DOPr internalization, although to a lesser degree than BMS 986187, suggesting that the modulator is promoting constitutive internalization of DOPr in these cells

(Trapaidze et al., 2000; Ong et al., 2015). This agrees with the BMS-986187-induced enhancement of DOPr internalization shown in Figure 3.

3.6. BMS 986187 induces low levels of DOPr phosphorylation and desensitization

DOPr phosphorylation, arrestin recruitment and receptor internalization are initiated by a phosphorylation event at Ser363 in the C-tail of DOPr (Kouhen et al., 2000; Qiu et al., 2007). As BMS 986187 promotes only a low level of receptor internalization or β-arrestin 2 recruitment, we hypothesized this was due to inefficient phosphorylation of this residue. To assess this, we performed western blot analysis of Ser363 phosphorylation of FLAG-tagged DOPr expressed in HEK 293 cells treated with various DOPr agonists for one h as shown in Figure 8. Consistent with the internalization data, BMS 986187 did not induce significant phosphorylation of this residue compared to the vehicle control. Similar findings were seen with TAN-67, whereas the higher internalizing agonists DPDPE and SNC80 caused a marked degree of phosphorylation.

Since BMS 986187 induced only a low level of receptor phosphorylation, arrestin recruitment and internalization, we predicted there would be a reduced DOPr desensitization, measured as a loss of receptor signaling, when cells were treated with BMS 986187 compared with SNC80. CHO hDOPr cells were incubated for varying times with equipotent concentrations (as determined by GTPγ^{35}S binding, Figure 1) of 10 μM BMS-986187 or 500 nM SNC80. Membranes homogenates were then prepared and GTPγ^{35}S binding determined following a

challenge with a maximal concentration (10μM) of SNC80. Membranes from cells pretreated with SNC80 or BMS 986187 showed a reduction in the maximal GTPγ^{35}S response, but the loss was more rapid for SNC80 (Figure 9), such that a one h pretreatment with SNC80 resulted in a 86% loss compared to only a 39 % loss with BMS 986187. Likewise, pre-incubation of cells for 30 min with BMS 986187 caused a lesser effect on the concentration response curve for SNC80 (maximum response = 68 ± 7%; EC_{50} = 7.4 ± 1.6 nM) than pre-incubation with SNC80 (maximal response = 31 ± 7%; EC50 = 25 ± 3.5 nM).

Discussion

The data presented indicate that BMS 986187 is a biased allosteric agonist at the DOPr receptor, giving a maximal response in the GTPγ^{35}S assay of equivalent magnitude to that seen with the orthosteric full agonist SNC80, albeit BMS 986187 is considerably less potent. In contrast to this strong response observed in G protein activation, BMS 986187 does not significantly recruit β-arrestin 2. This is a consequence of low levels of receptor phosphorylation and leads to a low level of receptor internalization and desensitization. When compared to SNC80, BMS 986187 is significantly biased toward G protein activation relative to recruitment of β-arrestin 2. This is the first evidence of an allosteric agonist displaying bias at an opioid receptor.

The direct agonist activity of BMS 986187 in the GTPγ^{35}S assay in HEK DOPr cells agrees with the results from the original report of PAMs at the DOPr using adenylyl cyclase inhibition in CHO cells as a readout (Burford et al., 2015). The allosteric nature of the observed agonism was suggested by the inability of BMS 986187 to compete with the orthosteric ligand ^{3}H-diprenophine (Burford et al., 2015). In the present study we confirm that BMS 986187 agonist activity occurs via binding to an allosteric site because the orthosteric antagonists NTI and naloxone only partially inhibit the ability of BMS986187 to stimulate GTPγ^{35}S binding, and increasing concentrations of the NTI do not give parallel shifts in the BMS 986187 concentration-response curve. This verifies that agonism can be mediated by sites on the receptor other than the orthosteric site and demonstrates an indirect interaction between the allosteric and the orthosteric sites. While these results in transfected HEK cells are encouraging, DOPrs are expressed at supraphysiological levels, which may not translate to relevant *in vivo* agonism (Langmead and Christopoulos, 2006; Kelly, 2013). Using mouse brain homogenates, we verified that the level of G protein activation elicited by BMS 986187 is similar to the full agonist, SNC80. However, these data also indicated that BMS 986187 is not completely selective for DOPr, since the same assay performed using mouse brain homogenates from DOPr knockout mice, still afforded a low level of GTPγ^{35}S stimulation. Previous work has indicated that BMS 986187 can act as a PAM for the MOPr and kappa opioid receptors, although no significant direct ago-PAM activity has so far been detected at either of these receptors

(Livingston et al., 2018). Alternatively, BMS 986187 could be acting at another, so far unidentified GPCR.

Despite stimulating a higher level of GTPγ^{35}S binding than the DOPr peptidic agonist DPDPE, BMS 986187 produced significantly lower receptor internalization. Thus, maximal G protein stimulation was in the order BMS 986187 = SNC80 > DPDPE > TAN-67 whereas maximal internalization was in the order SNC80 = DPDPE > TAN-67 = BMS 986187. This striking change of order of maximal effect across the two different signaling outputs using the same cell line indicates bias resulting from BMS 986187 occupancy of its allosteric binding site. We confirmed this finding by calculating the degree of bias for the signaling preference of BMS 986187-occupied DOPr for G protein activation versus β-arrestin 2 recruitment compared to SNC80 as a reference ligand. The very low level of β-arrestin 2 recruitment by BMS 986187 was confirmed by the lack of observable recruitment of GFP-labelled β-arrestin 2 to the plasma membrane in DOPr expressing HEK cells.

Comparing β-arrestin recruitment using the Presto Tango assay with GTPγ^{35}S binding we find DPDPE to be G protein biased at DOPr expressed in HEK cells, relative to SNC80. This agrees with studies that indicate SNC80 is a "super recruiter" of β-arrestin 2 relative to DPDPE at DOPr in CHO cells, whereas both have similar activity as inhibitors of AC (Chiang et al., 2016) and with predictions from studies *in vivo* that SNC80 is a "high-internalizing agonist" when compared to the low internalizing delta agonist ARM390 and partial agonists such as TAN67 (Pradhan et al., 2009, 2010; Pradhan et al., 2012). In contrast, bias calculations (Charfi et

al., 2015) based on data obtained at the DOPr expressed in HEK cells (Charfi et al., 2013), suggest SNC80 is highly biased towards AC inhibition relative to internalization when compared to DPDPE, although these data also show that SNC80 recruits much more β-arrestin than DPDPE. Overall, these findings highlight the importance of understanding the relativity of bias, where the chosen reference ligand can have a significant impact on the direction, magnitude and interpretation of observed results. Here, we chose to use SNC80 as a reference ligand as it is a "standard" DOPr ligand characterized in many *in vitro* and behavioral assays (Jutkiewicz et al., 2005; Danielsson et al., 2006; Pradhan et al., 2010; Chu Sin Chung et al., 2015; Dripps et al., 2017). On the other hand, we have shown DPDPE to be 11-fold biased towards G protein relative to β-arrestin recruitment using SNC80 as a reference, Consequently, if DPDPE is used as a reference ligand the bias of BMS 986187 towards G protein activation is reduced to 9-fold.

BMS 986187 also failed to afford DOPr-mediated phosphorylation of ERK1/2 in the MAP kinase pathway, despite showing significant G protein activation. This implies phosphorylation of ERK 1/2 *via* the allosteric site on DOPr may be a β-arrestin 2 mediated process, a ligand dependent effect observed at other GPCRs (Shukla et al., 2008). However, this contrasts with the finding that BMS 986187 when acting as a PAM for DOPr promotes ERK1/2 phosphorylation (Burford et al., 2015). This apparently conflicting data implies that the BMS 986187-occupied DOPr may signal differently depending on whether or not the orthosteric site is occupied. We are currently investigating the effect of BMS 986187 on ERK1/2 phosphorylation using a variety of DOPr agonists. PAM activity arises at opioid receptors by a negative indirect

action with the Na^+ ion binding site. Na^+ holds the receptor in inactive conformations (R) and loss of Na+ ion binding allows the receptor to adopt ensembles of active receptor (R*) states (Pert et al., 1973; Liu et al., 2012; Livingston and Traynor, 2014). PAMs with greater efficacy to displace Na^+ ion would then be predicted to show allosteric agonism by the same process. However, driving receptor activation through an allosteric site, there is no a priori reason why an allosteric agonist could not show functional selectivity at DOPr by promoting a different ensemble of R* conformations than an orthosteric ligand. Indeed, such an effect has been observed at the mAChr where allosteric agonists promoted bias when comparing G protein activation and ERK 1/2 phosphorylation (Gregory et al., 2010).

Recruitment of β-arrestin and DOPr internalization requires sequential phosphorylation of several Ser and Thr residues in the C terminal tail of the receptor by G protein receptor kinases (GRKs) (Stoffel et al., 1997; Ferguson, 2001; Qiu et al., 2007). Mutagenesis studies have indicated that an important initial phosphorylation site in the DOPr phosphorylation cascade is Ser363 (Kouhen et al., 2000). BMS 986187 produced a low level of Ser363 phosphorylation relative to DPDPE and SNC80 and similar to the low internalizing agonist TAN-67. This explains why the allosteric agonist shows significantly less desensitization than SNC80. However, it is perhaps surprising given the low level of phosphorylation and β-arrestin recruitment that BMS-986187 caused DOPr desensitization. It is possible that over extended periods, even with limited phosphorylation and β-arrestin recruitment, BMS 986187 is able to drive significant desensitization. Alternatively, the BMS 986187-occupied DOPr is in different

conformational states to an orthosteric agonist-occupied DOPr and so may employ different desensitization mechanisms. In this regard it should be noted that mutants of DOPr expressed in HEK cells showing no detectable phosphorylation still desensitize over time (El-Kouhen et al., 2000). Nonetheless, the low level of phosphorylation observed establishes that the bias driven by BMS 986187 results from reduced phosphorylation of the receptor, even though BMS 986187 does recruit G protein and presumably G protein receptor kinases. This signifies that DOPr conformations induced in the presence of BMS 986187 differ from those adopted in the presence of SNC80. A greater understanding of these conformations would provide insight into the driving force behind G protein versus β-arrestin mediated signaling for both orthosteric and allosteric ligands.

In conclusion, BMS 986187 is a biased allosteric agonist of the DOPr. Biased allosteric agonism at DOPr could represent a novel strategy for treating chronic pain and depression while potentially avoiding limiting factors such as rapid tolerance development and induction of convulsions.

Author Contributions

MAS and JRT designed experiments and analyzed data. MAS, KEL, LC performed experiments and analyzed data. ZW performed and analyzed ERK1/2 experiments with supervision from

MP. MAS and JRT wrote the manuscript. JRT provided funding and supervision for the overall project.

Acknowledgements

This work was supported by a grant from the National Institutes of Health USA (R37 DA39997 to JRT). MAS was also supported by NIH training grant (T32 GM007767).

Conflict of interest

The authors declare no conflicts of interest

Declaration of transparency and scientific rigour

This Declaration acknowledges that this paper adheres to the principles for transparent reporting and scientific rigour of preclinical research as stated in the *BJP* guidelines for Design & Analysis, Immunoblotting and Immunochemistry, and Animal Experimentation, and as recommended by funding agencies, publishers and other organisations engaged with supporting research.

References

Alexander SPH, Christopoulos A, Davenport AP, Kelly E, Marrion NV, Peters JA, Faccenda

E, Harding SD, Pawson AJ, Sharman JL, Southan C, Davies JA; CGTP Collaborators. (2017) The Concise Guide to PHARMACOLOGY 2017/18: G protein-coupled receptors. Br J Pharmacol. 174 Suppl 1: S17-S129.

Audet, N., Galés, C., Archer-Lahlou, É., Vallières, M., Schiller, P.W., Bouvier, M., et al. (2008). Bioluminescence resonance energy transfer assays reveal ligand-specific conformational changes within preformed signaling complexes containing δ-opioid receptors and heterotrimeric G proteins. J. Biol. Chem. *283*: 15078–15088.

Bie, B., and Pan, Z.Z. (2007). Trafficking of central opioid receptors and descending pain inhibition. Mol. Pain *3*: 37.

Bradbury, F.A., Zelnik, J.C., and Traynor, J.R. (2009). G Protein independent phosphorylation and internalization of the δ-opioid receptor. J. Neurochem. *109*: 1526–1535.

Burford, N.T., Livingston, K.E., Canals, M., Ryan, M.R., Budenholzer, L.M.L., Han, Y., et al. (2015a). Discovery, synthesis, and molecular pharmacology of selective positive allosteric modulators of the δ-opioid receptor. J. Med. Chem. *58*: 4220–4229.

Burford, N.T., Traynor, J.R., and Alt, A. (2015b). Positive allosteric modulators of the μ-opioid receptor: A novel approach for future pain medications. Br. J. Pharmacol. *172*: 277–286.

Cahill, C.M., Holdridge, S. V., and Morinville, A. (2007). Trafficking of δ-opioid receptors and other G-protein-coupled receptors: implications for pain and analgesia. Trends Pharmacol. Sci. *28*: 23–31.

Che, T., Majumdar, S., Zaidi, S.A., Ondachi, P., McCorvy, J.D., Wang, S., et al. (2018). Structure of the Nanobody-Stabilized Active State of the Kappa Opioid Receptor. Cell *172*: 55–67.e15.

Chiang, T., Sansuk, K., and Rijn, R.M. van (2016). beta-Arrestin 2 dependence of delta opioid receptor agonists is correlated with alcohol intake. Br. J. Pharmacol. *173*: 332–343.

Chu Sin Chung, P., Boehrer, A., Stephan, A., Matifas, A., Scherrer, G., Darcq, E., et al. (2015). Delta opioid receptors expressed in forebrain GABAergic neurons are responsible for SNC80-induced seizures. Behav. Brain Res. *278*: 429–434.

Clark, M.J., Harrison, C., Zhong, H., Neubig, R.R., and Traynor, J.R. (2003). Endogenous RGS protein action modulates δ-opioid signaling through Gio: Effects on adenylyl cyclase, extracellular signal-regulated kinases, and intracellular calcium pathways. J. Biol. Chem. *278*: 9418–9425.

Conn, P.J., Christopoulos, A., and Lindsley, C.W. (2010). Allosteric modulators of GPCRs: a novel approach for the treatment of CNS disorders. Nat. Rev. Drug Discov. *8*: 41–54.

Curtis, M.J., Bond, R.A., Spina, D., Ahluwalia, A., Alexander, S.P.A., Giembycz, M.A., et al. (2015). Experimental design and analysis and their reporting: new guidance for publication in BJP. Br. J. Pharmacol. *172*: 3461–3471.

Danielsson, I., Gasior, M., Stevenson, G.W., Folk, J.E., Rice, K.C., and Negus, S.S. (2006). Electroencephalographic and convulsant effects of the delta opioid agonist SNC80 in rhesus

monkeys. Pharmacol. Biochem. Behav. *85*: 428–434.

Dripps, I.J., Boyer, B.T., Neubig, R.R., Rice, K.C., Traynor, J.R., and Jutkiewicz, E.M. (2017). Role of signaling molecules in behaviors mediated by the δ-receptor agonist SNC80. Br. J. Pharmacol. *175*: 891-901.

El Kouhen, O.M., Wang, G., Solberg, J., Erickson, L.J., Law, P.Y., and Loh, H.H. (2000). Hierarchical phosphorylation of δ-opioid receptor regulates agonist-induced receptor desensitization and internalization. J. Biol. Chem. *275*: 36659–36664.

Ferguson, S.S. (2001). Evolving concepts in G protein-coupled receptor endocytosis: the role in receptor desensitization and signaling. Pharmacol. Rev. *53*: 1–24.

Filliol, D., Ghozland, S., Chluba, J., Martin, M., Matthes, H.W.D., Simonin, F., et al. (2000). Mice deficient for δ- and μ-opioid receptors exhibit opposing alterations of emotional responses. Nat. Genet. *25*: 195–200.

Fritz, R.D., Letzelter, M., Reimann, A., Martin, K., Fusco, L., Ritsma, L., et al. (2013). A versatile toolkit to produce sensitive FRET biosensors to visualize signaling in time and space. Sci. Signal. *6*: 1–14.

Gregory, K.J., Hall, N.E., Tobin, A.B., Sexton, P.M., and Christopoulos, A. (2010). Identification of orthosteric and allosteric site mutations in M2 muscarinic acetylcholine receptors that contribute to ligand-selective signaling bias. J. Biol. Chem. *285*: 7459–7474.

Harding SD, Sharman JL, Faccenda E, Southan C, Pawson AJ, Ireland S *et al.* (2018). The IUPHAR/BPS Guide to PHARMACOLOGY in 2018: updates and expansion to encompass the new guide to IMMUNOPHARMACOLOGY. Nucl Acids Res 46: D1091-D1106.

Jutkiewicz, E.M., Kaminsky, S.T., Rice, K.C., Traynor, J.R., and Woods, J.H. (2005). Differential behavioral tolerance to the delta-opioid agonist SNC80 ([(+)-4-[(alphaR)-alpha-[(2S,5R)-2,5-dimethyl-4-(2-propenyl)-1-piperazinyl]-(3-methoxyphenyl)methyl]-N,N-diethylbenzamide) in Sprague-Dawley rats. J. Pharmacol. Exp. Ther. *315*: 414–422.

Kabli, N., and Cahill, C.M. (2007). Anti-allodynic effects of peripheral delta opioid receptors in neuropathic pain. Pain *127*: 84–93.

Kelly, E. (2013). Efficacy and ligand bias at the δ-opioid receptor. Br. J. Pharmacol. *169*: 1430–1446.

Kenakin, T. (2007). Allosteric Agonist Modulators. J. Recept. Signal Transduct. *27*: 247–259.

Kenakin, T. (2017). A System-independent Scale of Agonism and Allosteric Modulation for Assessment of Selectivity, Bias and Receptor Mutation. Mol. Pharmacol.

Kenakin, T., and Christopoulos, A. (2013). Signalling bias in new drug discovery: detection, quantification and therapeutic impact. Nat. Rev. Drug Discov. *12*: 205–16.

Kenakin, T., Watson, C., Muniz-Medina, V., Christopoulos, A., and Novick, S. (2012). A simple method for quantifying functional selectivity and agonist bias. ACS Chem. Neurosci. *3*: 193–

203.

Keov, P., Sexton, P.M., and Christopoulos, A. (2011). Allosteric modulation of G protein-coupled receptors: a pharmacological perspective. Neuropharmacology *60*: 24–35.

Kessler, R.C., and Bromet, E.J. (2013). The epidemiology of depression across cultures. Annu. Rev. Public Health *34*: 119–138.

Kilkenny, C., Browne, W.J., Cuthill, I.C., Emerson, M., and Altman, D.G. (2010). Improving Bioscience Research Reporting: The ARRIVE Guidelines for Reporting Animal Research. PLOS Biol. *8*: e1000412.

Langmead, C.J., and Christopoulos, A. (2006). Allosteric agonists of 7TM receptors: expanding the pharmacological toolbox. Trends Pharmacol. Sci. *27*: 475–481.

Lester, P.A., and Traynor, J.R. (2006). Comparison of the in vitro efficacy of mu, delta, kappa and ORL1 receptor agonists and non-selective opioid agonists in dog brain membranes. Brain Res. *1073–1074*: 290–6.

Liu, W., Chun, E., Thompson, A.A., Chubukov, P., Xu, F., Katritch, V., et al. (2012). Structural basis for allosteric regulation of GPCRs by sodium ions. Science *337*: 232–236.

Livingston, K.E., Stanczyk, M.A., Burford, N.T., Alt, A., Canals, M., and Traynor, J.R. (2018). Pharmacologic Evidence for a Putative Conserved Allosteric Site on Opioid Receptors. Mol. Pharmacol. *93*: 157–167.

Livingston, K.E., and Traynor, J.R. (2014). Disruption of the Na + ion binding site as a mechanism for positive allosteric modulation of the mu-opioid receptor. Proc. Natl. Acad. Sci. *111*: 18369–18374.

Lutz, Pierre-Eric and Brigitte, K. (2014). Opioid receptors □: distinct roles in Trends Neurosci. *36*: 195–206.

McGrath, J.C., and Lilley, E. (2015). Implementing guidelines on reporting research using animals (ARRIVE etc.): new requirements for publication in BJP. Br. J. Pharmacol. *172*: 3189–3193.

McNicol, E., Horowicz-Mehler, N., Fisk, R.A., Bennett, K., Gialeli-Goudas, M., Chew, P.W., et al. (2017). Management of opioid side effects in cancer-related and chronic noncancer pain: a systematic review. J. Pain *4*: 231–256.

Ong, E.W., Xue, L., Olmstead, M.C., and Cahill, C.M. (2015). Prolonged morphine treatment alters δ opioid receptor post-internalization trafficking. Br. J. Pharmacol. *172*: 615–629.

Pert, C.B., Pasternak, G., and Snyder, S.H. (1973). Opiate agonists and antagonists discriminated by receptor binding in brain. Science *182*: 1359–1361.

Pradhan, A.A., Befort, K., Nozaki, C., Gavériaux-Ruff, C., and Kieffer, B.L. (2011). The delta opioid receptor: an evolving target for the treatment of brain disorders. Trends Pharmacol. Sci. *32*: 581–590.

Pradhan, A.A., Smith, M.L., Kieffer, B.L., and Evans, C.J. (2012). Ligand-directed signalling within the opioid receptor family. Br. J. Pharmacol. *167*: 960–969.

Pradhan, A.A.A., Becker, J.A.J., Scherrer, G., Tryoen-Toth, P., Filliol, D., Matifas, A., et al. (2009). In vivo delta opioid receptor internalization controls behavioral effects of agonists. PLoS One *4*: e5425.

Pradhan, A.A.A., Walwyn, W., Nozaki, C., Filliol, D., Erbs, E., Matifas, A., et al. (2010). Ligand-directed trafficking of the delta-opioid receptor in vivo: two paths toward analgesic tolerance. J. Neurosci. *30*: 16459–16468.

Przewłocki, R., and Przewłocka, B. (2001). Opioids in chronic pain. Eur. J. Pharmacol. *429*: 79–91.

Qiu, Y., Loh, H.H., and Law, P.-Y. (2007). Phosphorylation of the delta-opioid receptor regulates its beta-arrestins selectivity and subsequent receptor internalization and adenylyl cyclase desensitization. J. Biol. Chem. *282*: 22315–22323.

Reinke, T. (2014). Providers need to boost efforts to prevent abuse of narcotics. Manag. Care *23*: 11–12.

Rush, A.J., Trivedi, M.H., Wisniewski, S.R., Nierenberg, A.A., Stewart, J.W., Warden, D., et al. (2006). Acute and longer-term outcomes in depressed outpatients requiring one or several treatment steps: a STAR*D report. Am. J. Psychiatry *163*: 1905–1917.

Saitoh, A., and Yamada, M. (2012). Antidepressant-like Effects of δ Opioid Receptor Agonists in Animal Models. Curr. Neuropharmacol. *10*: 231–8.

Schmid, C.L., Kennedy, N.M., Ross, N.C., Lovell, K.M., Yue, Z., Morgenweck, J., et al. (2017). Bias Factor and Therapeutic Window Correlate to Predict Safer Opioid Analgesics. Cell *171*: 1165.e13-1170.

Shiwarski, D.J., Darr, M., Telmer, C.A., Bruchez, M.P., and Puthenveedu, M.A. (2017). PI3K Class II α regulates δ-Opioid Receptor Export from the *trans* -Golgi Network. Mol. Biol. Cell mbc.E17-01-0030.

Shukla, A.K., Violin, J.D., Whalen, E.J., Gesty-palmer, D., Shenoy, S.K., and Lefkowitz, R.J. (2008). Distinct conformational changes in -arrestin report biased agonism at seven-transmembrane receptors.

Stoffel, R.H. 3rd, Pitcher, J.A., and Lefkowitz, R.J. (1997). Targeting G protein-coupled receptor kinases to their receptor substrates. J. Membr. Biol. *157*: 1–8.

Trapaidze, N., Gomes, I., Bansinath, M., and Devi, L.A. (2000). Recycling and Resensitization of Delta Opioid Receptors. DNA Cell Biol. *19*: 10.1089/104454900314465.

Traynor, J.R., and Nahorski, S.R. (1995). Modulation by mu-opioid agonists of guanosine-5'-O-(3-[35S]thio)triphosphate binding to membranes from human neuroblastoma SH-SY5Y cells. Mol. Pharmacol. *47*: 848–54.

Tryoen-Toth, P., Decaillot, F.M., Filliol, D., Befort, K., Lazarus, L.H., Schiller, P.W., et al. (2005). Inverse agonism and neutral antagonism at wild-type and constitutively active mutant delta opioid receptors. J Pharmacol Exp Ther *313*: 410–421.

Weinberg, Z.Y., Zajac, A.S., Phan, T., Shiwarski, D.J., and Puthenveedu, M.A. (2017). Sequence-Specific Regulation of Endocytic Lifetimes Modulates Arrestin-Mediated Signaling at the μ Opioid Receptors. Mol. Pharmacol. Mol Pharmacol *91*: 416–427.

Whalen, E.J., Rajagopal, S., and Lefkowitz, R.J. (2011). Therapeutic potential of β-arrestin- and G protein-biased agonists. Trends Mol. Med. *17*: 126–139.

Figure Legends

Figure 1. BMS 986187 elicits G protein activation. The capacity for increasing concentrations of BMS 9861897 and SNC80 to increase GTPγ^{35}S binding was measured in membranes from FLAG-tagged HEK hDOPr cells (A) or in brain homogenates from wild type or DOPr knockout (KO) mice (B). Data are presented as percentage of the response to a maximal concentration (10μM) of SNC80. All plotted points are the means ± SEM of five independent experiments, each run in duplicate.

Figure 2. Antagonists show non-competitive interaction with BMS 986187. (A) Antagonists naltrindole (NTI) and naloxone (NLX) reduce maximal GTPγ^{35}S binding caused by BMS 986187 in FLAG-tagged HEK hDOPr cells, normalized to percent of effect of 10 μM SNC80 to control for variation between the different preparations. (B) GTPγ^{35}S concentration response curves for BMS 986187 with increasing NTI concentrations and (C) GTPγ^{35}S binding concentration response of NTI with fixed concentration BMS 986187 (10 μM) or SNC80 (1 μM), in CHO cells expressing hDOPr. All plotted points are the mean ± SEM of five (B, C) or ten (A) individual experiments, each performed in duplicate.

Figure 3. DOPr Internalization. Receptor internalization by DOPr ligands in HEK cells expressing FLAG-tagged hDOPr. Preliminary time-course studies (means ± SEM, n = 3 experiments in triplicate) with 10 μM concentrations of ligands (A) were to identify an appropriate time (1 h) to determine (B) concentration-response studies for the different DOPr ligands (means ± SEM, n = 5 experiments in triplicate). The symbols in (A) also refer to (B).

Figure 4. BMS 986187 shows biased activation of GTPγ^{35}S relative to receptor internalization. DOPr ligands were evaluated in FLAG-tagged HEK hDOPr cells by measuring (A) receptor internalization or (B) stimulation of GTPγ^{35}S bound. BMS 986187 showed significantly lower internalization relative to DPDPE and SNC80, despite showing significantly greater GTPγ^{35}S

binding relative to TAN-67 and DPDPE. GTPγ^{35}S binding is normalized as percent of 10 μM SNC80 to control for variation between the different preparations. All experiments were performed using saturating concentrations of compounds (10μM). Data are expressed as mean ± SEM of five (internalization) or ten (GTPγ^{35}S) individual experiments, each performed in duplicate.

Figure 5. BMS 986187 is G protein biased over β-arrestin 2. BMS 986187 bias was evaluated between β-arrestin 2 recruitment (A) and GTPγ^{35}S binding (B) relative to the standard orthosteric agonist SNC80. Normalization was performed to control for sources of variation across preparation and to allow for comparison across both assays. β-arrestin assays were performed in HTLA cells transiently transfected with hDOR-TANGO and GTPγ^{35}S assays in membranes from HEK cells expressing FLAG-tagged hDOPr as described in the methods. Data are presented as the mean of five (GTPγ^{35}S) or seven (β-arrestin 2) independent experiments, each performed in duplicate and expressed as mean ± S.E.M.

Figure 6. Effect of SNC80 and BMS 986187 on β-arrestin 2 Recruitment. FLAG-tagged HEK hDOPr cells were transfected with 0.4 μg β-arrestin 2 GFP and treated with 10 μM of either SNC80 or BMS 986187 for five min and imaged using confocal microscopy. FLAG-tagged DOPr is represented in the red channel with the green channel representing β-arrestin 2. (A)

Representative images and (B) β-arrestin 2 recruitment expressed as surface/cytoplasmic GFP intensity. Data represent the means ± S.E.M. of 34 cells per condition from five independent drug treatments.

Figure 7. BMS 986187 elicits low ERK 1/2 phosphorylation. **(**A) Example montage of cytoplasmic ERK response in FLAG-tagged hDOPr expressing HEK 293 cells in response to 1μM SNC80. Top row: FLAG-tagged DOPr labeled with Alexa647-conjugated M1 Antibody. Bottom row: ratio of FRET/CFP fluorescence of expressed cEKAR sensor. Agonist added at 2.5 min. Scale bar is 20μm, frames every 4 min. (B) Representative montage of cytoplasmic ERK response measured in DOPr-expressing HEK 293 cell in response to 10μM BMS 986187. (C) Average ERK response over time of DOPr-expressing HEK 293 cells treated with either 1μM SNC80 (n=47 cells), 10 μM BMS 986187 (n=34 cells) or vehicle (n=39 cells). Responses are represented as fractional change over baseline. Solid line is the mean response, shaded region inside dotted lines represents ± SEM. (D) SNC80 produced a significantly higher total ERK response compared to BMS 986187. Total response is measured as area under curve of treatment condition minus area under curve of vehicle. Error bars represent means ± SEM.

Figure 8. BMS 986187 poorly phosphorylates Ser363 on DOPr. (A)Western Blot of FLAG-tagged HEK hDOPr membranes incubated with 10 μM concentrations of various DOPr ligands

probed for phosphorylated Ser363 (B) Data are expressed as a ratio of phosphorylated receptor to total receptor (FLAG). Each column is the mean of five independent experiments ± S.E.M.

Figure 9. BMS 986187 treatment produces significantly less loss of agonist activity at DOPr than SNC80. (A) CHO cells expressing the hDOPr were pretreated with either 500 nM SNC80 or 10 μM BMS 986187 for the indicated times and then membrane homogenates were prepared as described in the methods. The level of GTPγ^{35}S binding induced by 10μM SNC80 in the membranes was determined and plotted against the time of cell pretreatment with SNC80 or BMS-986187. (B) CHO cells expressing the hDOPr were pretreated as above with SNC80 or BMS 986187 for 30 mins, membranes homogenates prepared and SNC80 concentration response curves for stimulation of GTPγ^{35}S binding were constructed. Data are expressed as % of maximum binding in untreated cells ± S.E.M from five independent experiments, each performed in duplicate.

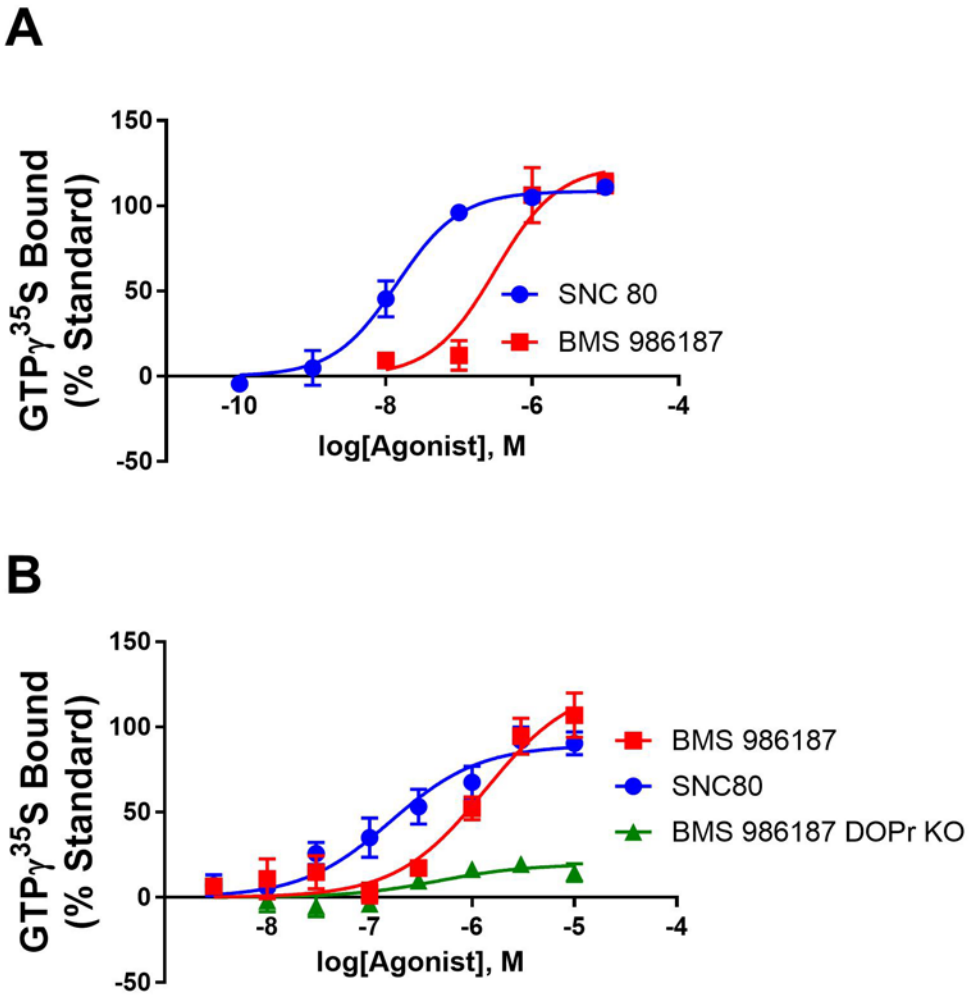

Figure 1.

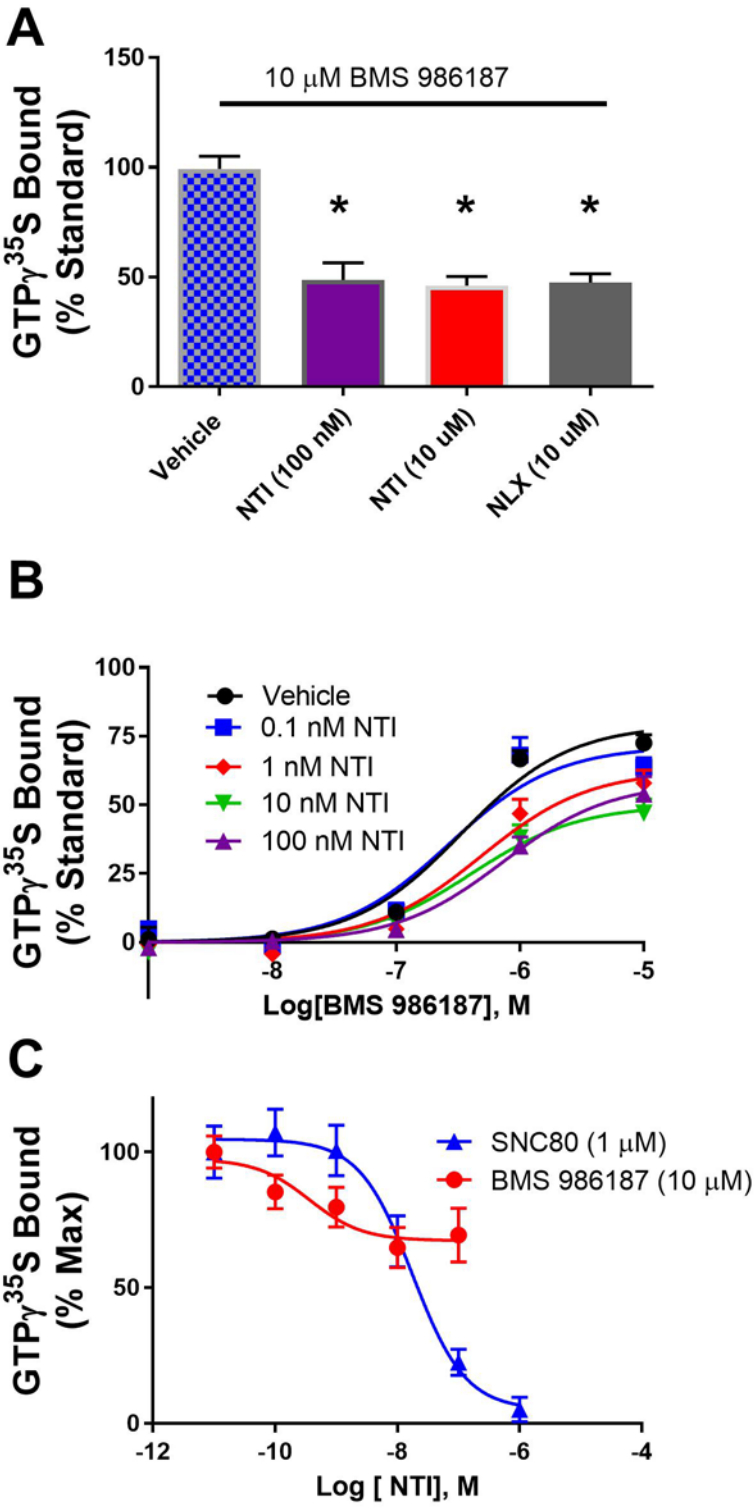

Figure 2

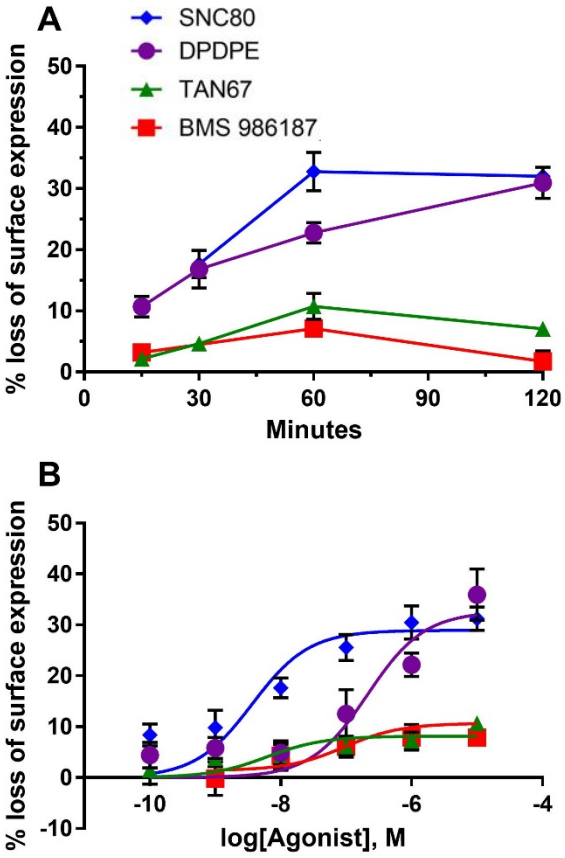

Figure 3

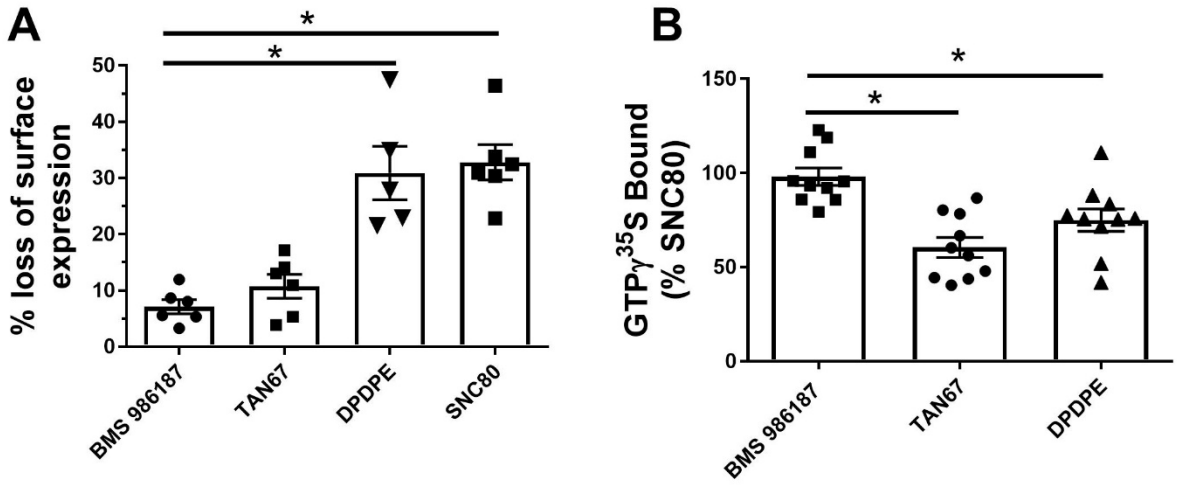

Figure 4

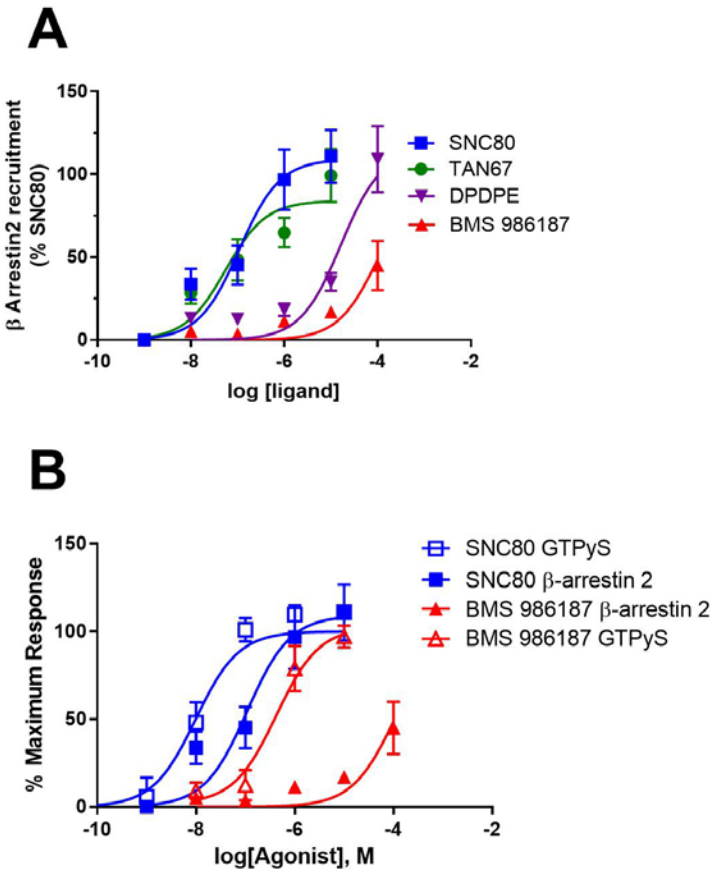

Figure 5.

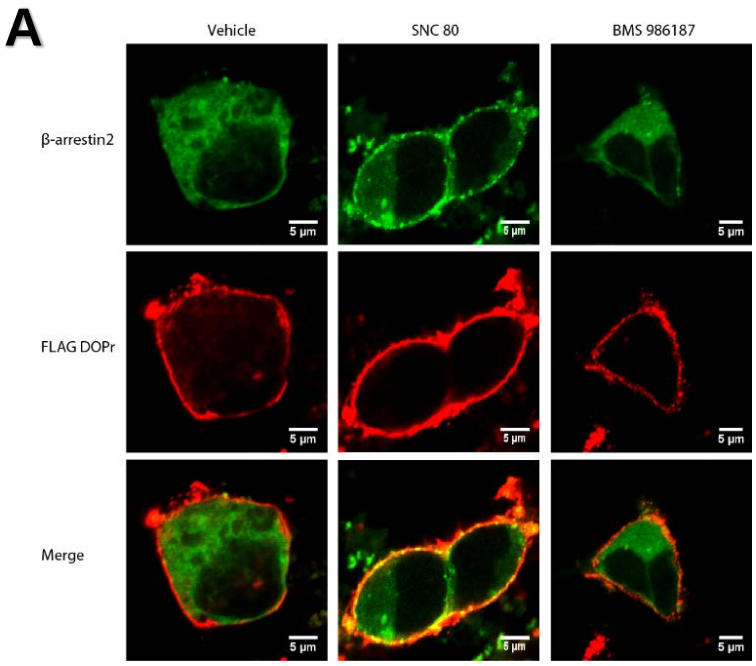

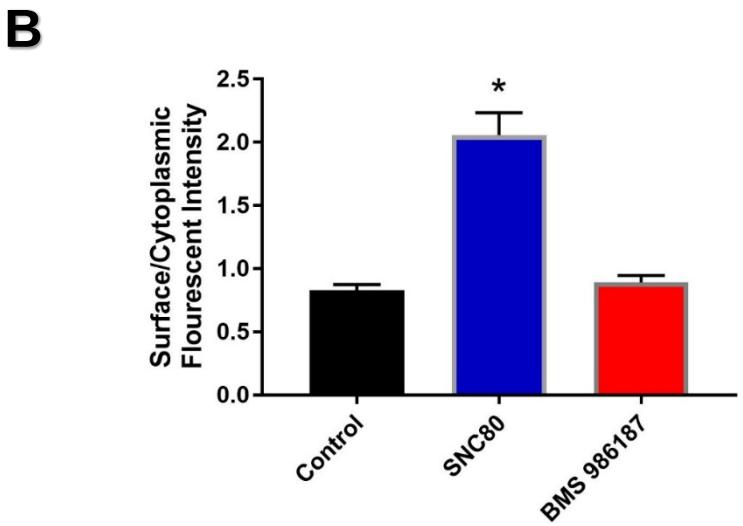

Figure 6.

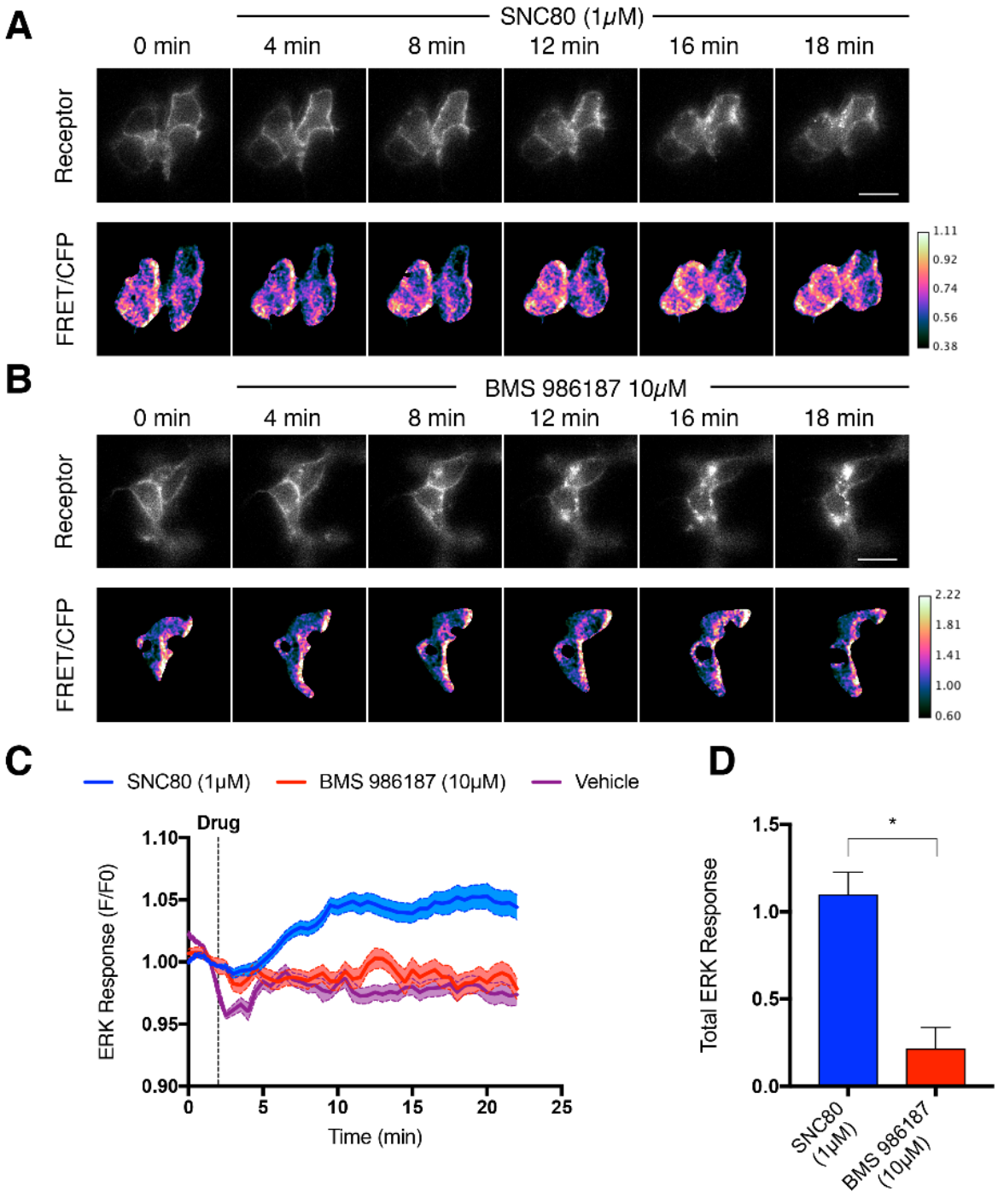

Figure 7.

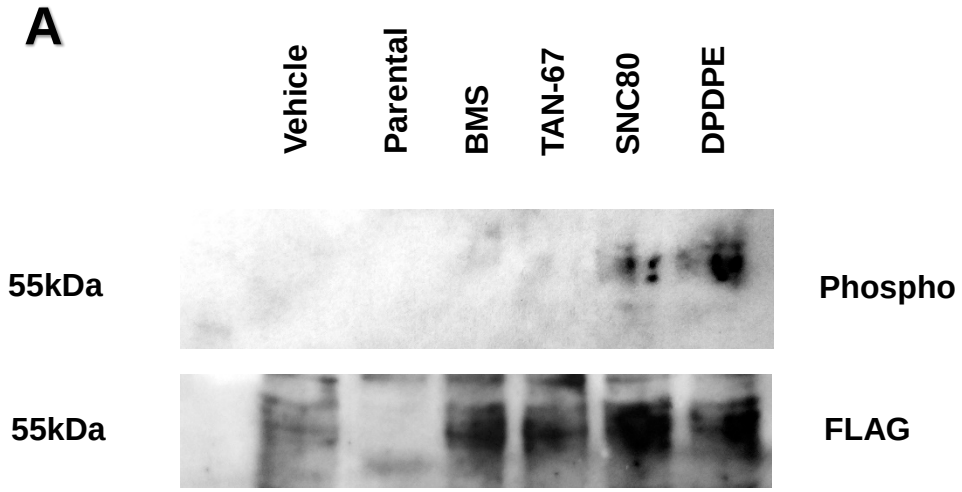

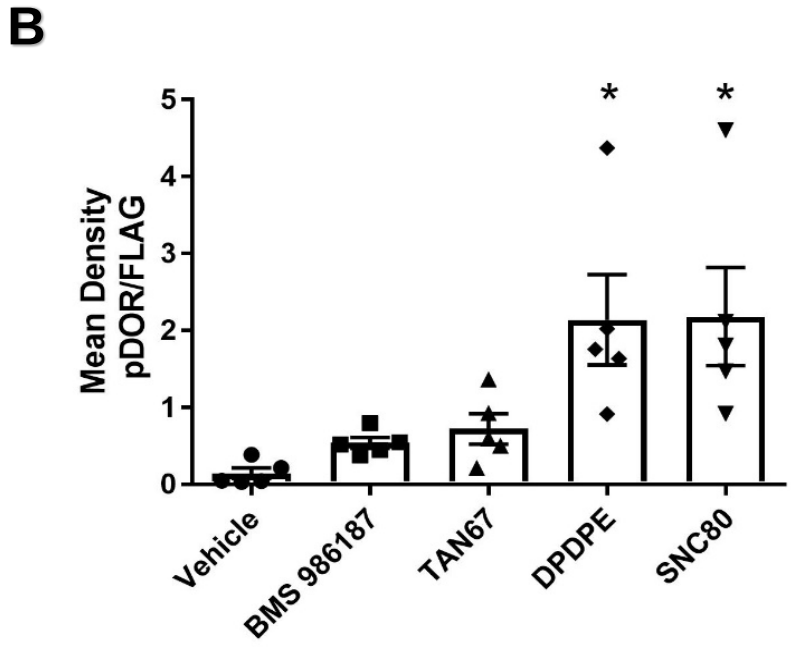

Figure 8.

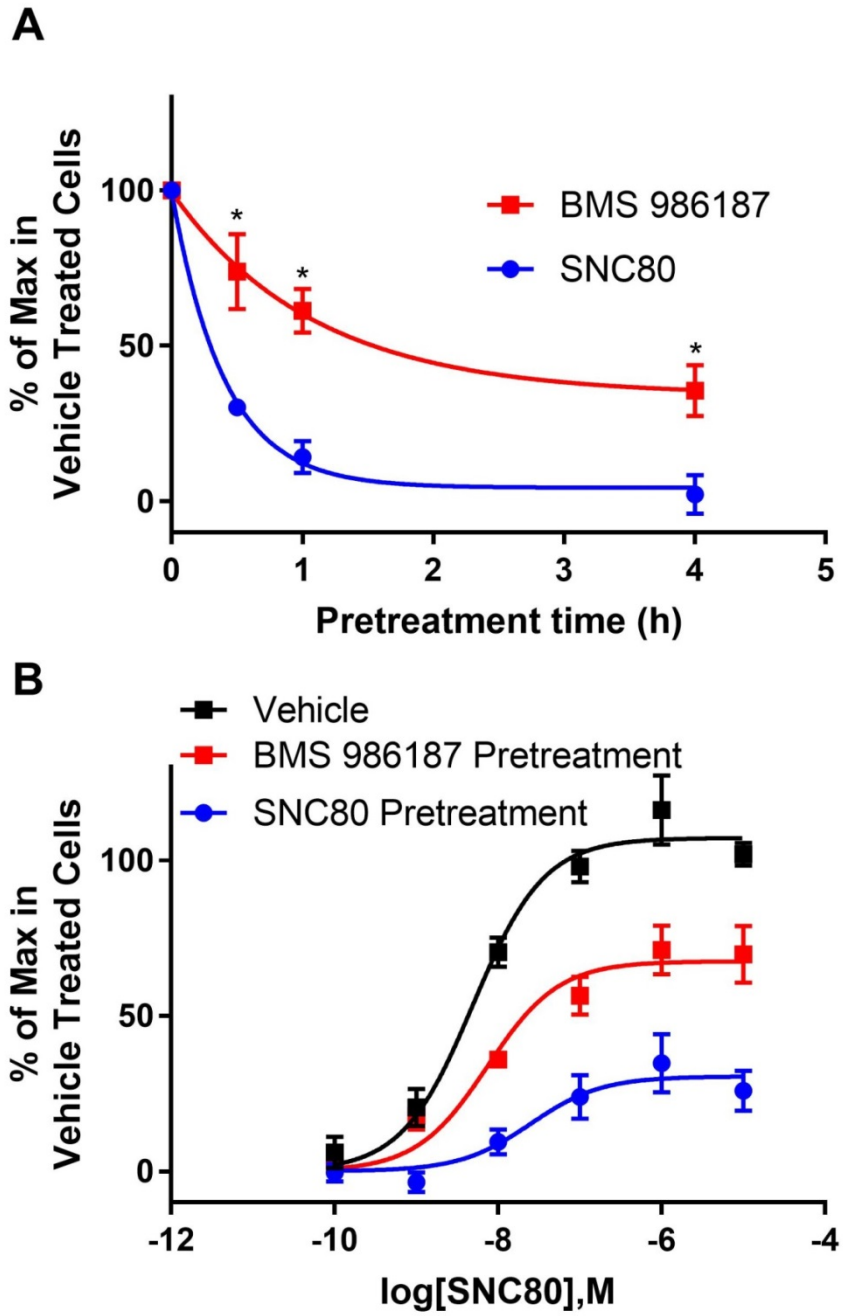

Figure 9.

	β-arrestin 2		Bias (Toward G protein)			$GTP\gamma^{35}S$	
	Max	EC_{50} (nM)	Arrestin/G protein Fold EC_{50} Shift	$\Delta\Delta\log(Max/EC_{50})$	Bias Factor	EC_{50} (nM)	Max
SNC80	1	353 ± 141	18.6	0	1	19.0 ± 6	1
BMS 986187	1* 0.5*	578,500 ± 419,100 238,179 ± 188,400	1787 737	1.91 ± 0.7 1.53 ± 0.82	81 34	323 ± 96	0.92 ± 0.03
DPDPE	1	16,100 ± 805	85	1.03 ± 0.67	11	189 ± 25	0.85 ± 0.09

Table 1. Summary of Bias Calculations. Calculations were performed from data generated in Figure 5, as described in the methods to determine $\Delta\Delta\log(max/EC_{50})$ (Kenakin, 2017). *In order to extrapolate an accurate EC_{50} value for BMS 986187-mediated arrestin recruitment, the E_{max} was constrained to 1, equivalent to the level of recruitment by SNC80 or 0.5, assuming the maximum value is that observed at the point of solubility (Figure. 5B).

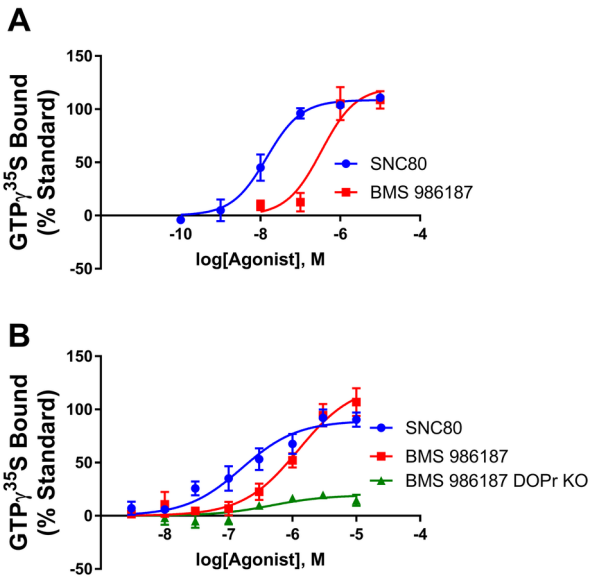

BPH_14602_Figure 1.tif

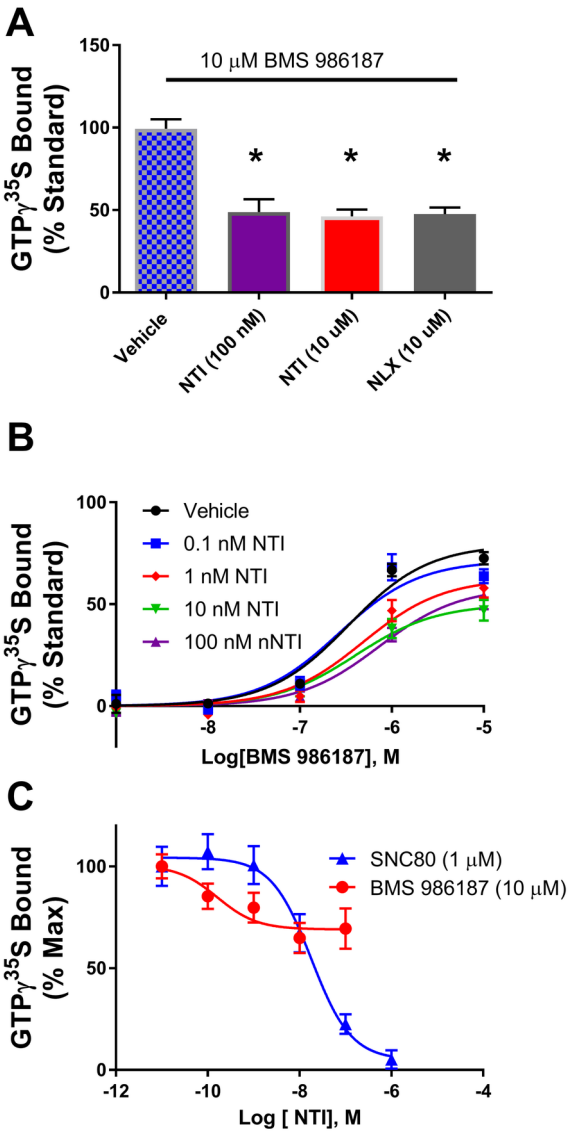

BPH_14602_Figure 2.tif

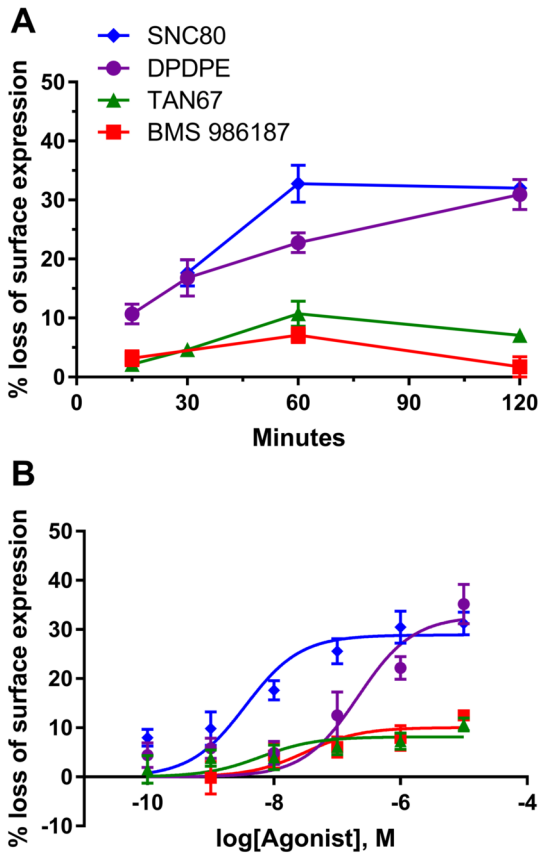

BPH_14602_Figure 3.tif

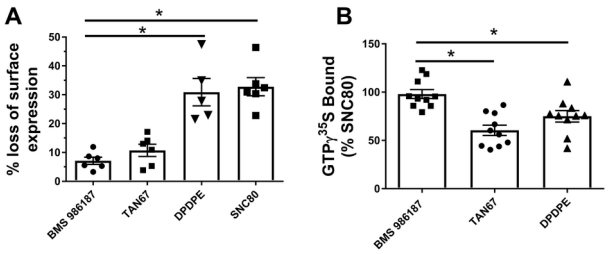

BPH_14602_Figure 4.tif

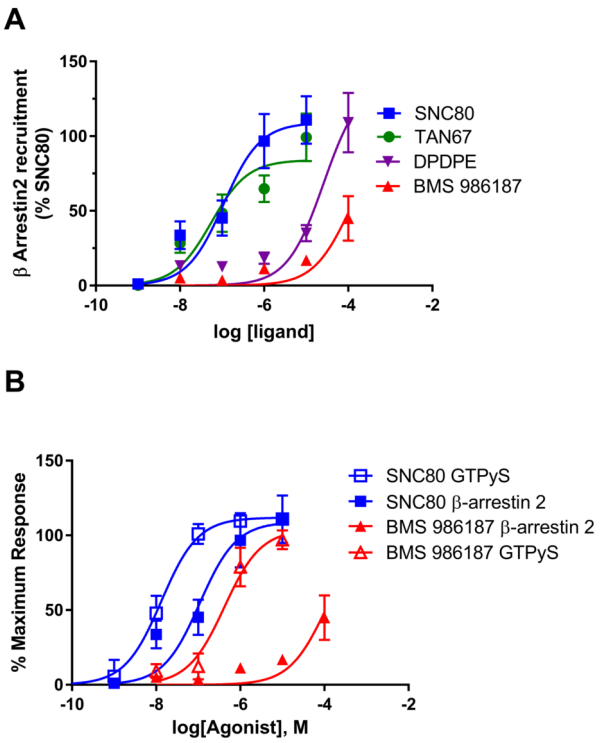

BPH_14602_Figure 5.tif

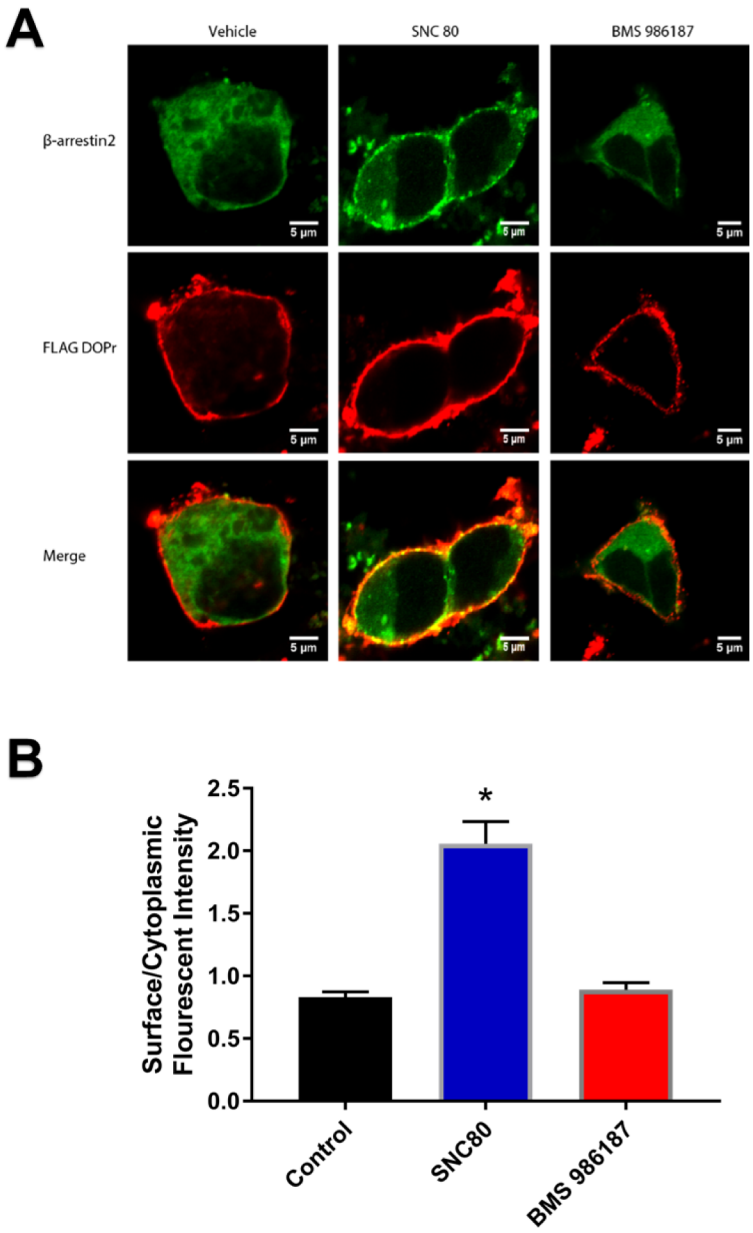

BPH_14602_Figure 6.tif

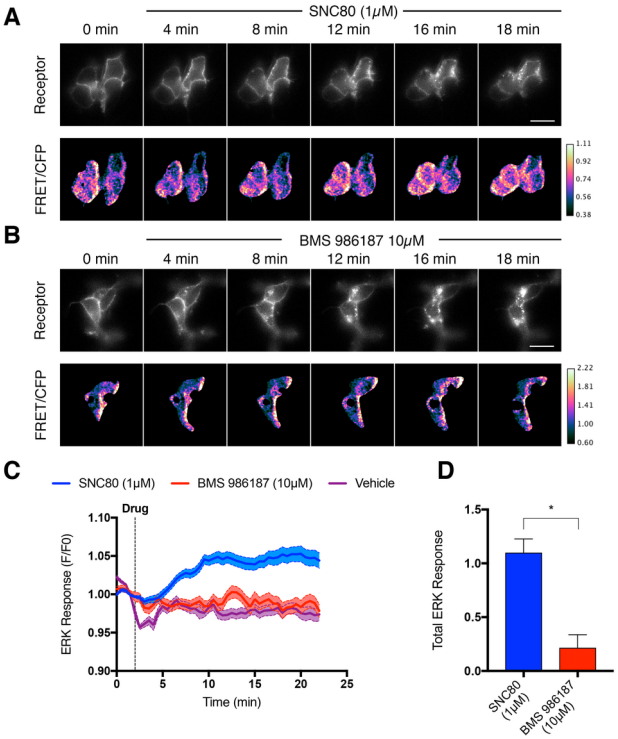

BPH_14602_Figure 7.tif

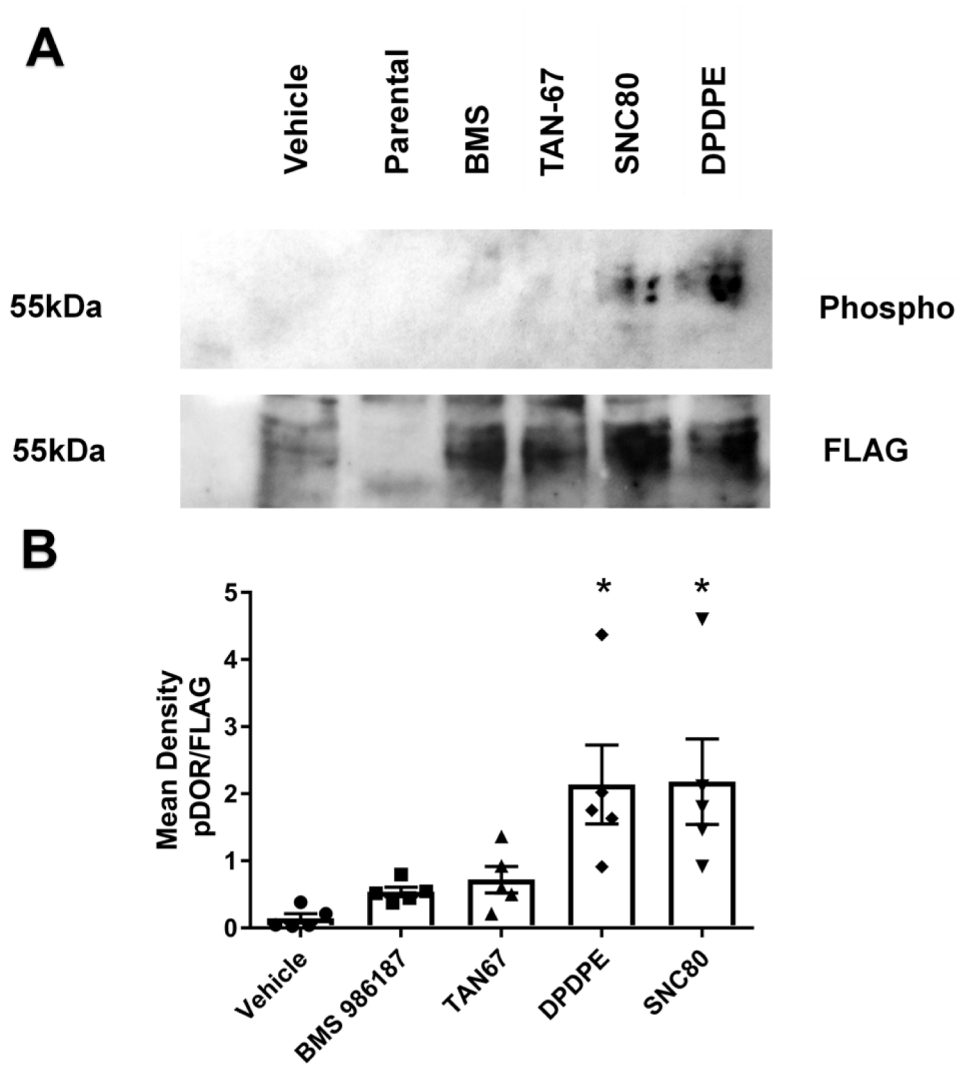

BPH_14602_Figure 8.tif

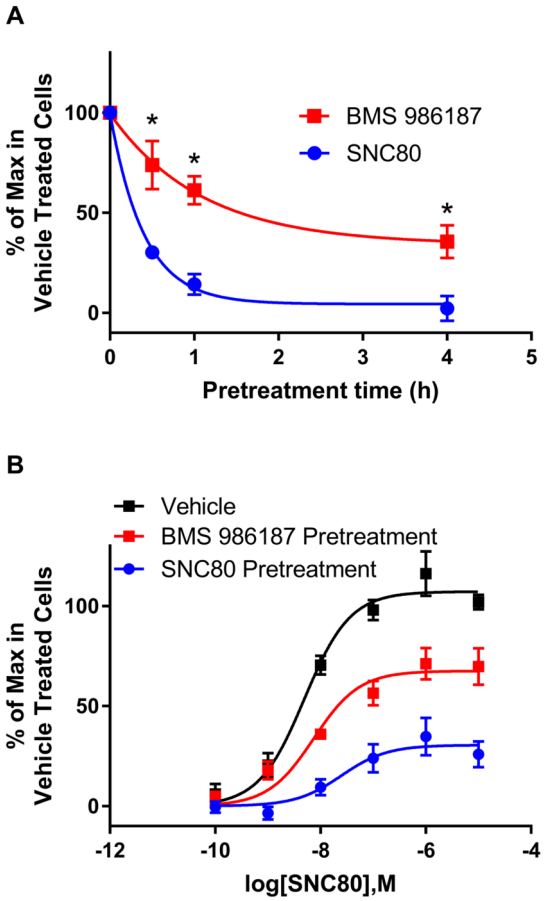

BPH_14602_Figure 9.tif